Photoaffinity labeling identifies an intersubunit steroid-binding site in heteromeric GABA type A (GABA_A) receptors

Selwyn S. Jayakar[1,‡], David C. Chiara[1,†,‡], Xiaojuan Zhou[2], Bo Wu[3], Karol S. Bruzik[3], Keith W. Miller[2], and Jonathan B. Cohen[1,*]

From the [1]Department of Neurobiology, Harvard Medical School, Boston, Massachusetts, the [2]Department of Anesthesia, Critical Care and Pain Medicine, Massachusetts General Hospital, Boston, Massachusetts, and the [3]Department of Medicinal Chemistry and Pharmacognosy, University of Illinois at Chicago, Chicago, Illinois

Edited by Karen G. Fleming

Allopregnanolone ($3\alpha5\alpha$-P), pregnanolone, and their synthetic derivatives are potent positive allosteric modulators (PAMs) of GABA_A receptors (GABA_ARs) with *in vivo* anesthetic, anxiolytic, and anti-convulsant effects. Mutational analysis, photoaffinity labeling, and structural studies have provided evidence for intersubunit and intrasubunit steroid-binding sites in the GABA_AR transmembrane domain, but revealed only little definition of their binding properties. Here, we identified steroid-binding sites in purified human $\alpha1\beta3$ and $\alpha1\beta3\gamma2$ GABA_ARs by photoaffinity labeling with [^{3}H]21-[4-(3-(trifluoromethyl)-3H-diazirine-3-yl) benzoxy]allopregnanolone ([^{3}H]21-pTFDBzox-AP), a potent GABA_AR PAM. Protein microsequencing established $3\alpha5\alpha$-P inhibitable photolabeling of amino acids near the cytoplasmic end of the β subunit M4 (β3Pro-415, β3Leu-417, and β3Thr-418) and M3 (β3Arg-309) helices located at the base of a pocket in the $\beta^+-\alpha^-$ subunit interface that extends to the level of αGln-242, a steroid sensitivity determinant in the αM1 helix. Competition photolabeling established that this site binds with high affinity a structurally diverse group of 3α-OH steroids that act as anesthetics, anti-epileptics, and anti-depressants. The presence of a 3α-OH was crucial: 3-acetylated, 3-deoxy, and 3-oxo analogs of $3\alpha5\alpha$-P, as well as 3β-OH analogs that are GABA_AR antagonists, bound with at least 1000-fold lower affinity than $3\alpha5\alpha$-P. Similarly, for GABA_AR PAMs with the C-20 carbonyl of $3\alpha5\alpha$-P or pregnanolone reduced to a hydroxyl, binding affinity is reduced by 1,000-fold, whereas binding is retained after deoxygenation at the C-20 position. These results provide a first insight into the structure-activity relationship at the GABA_AR $\beta^+-\alpha^-$ subunit interface steroid-binding site and identify several steroid PAMs that act via other sites.

Endogenous neurosteroids, including allopregnanolone ($3\alpha5\alpha$-P) and pregnanolone ($3\alpha5\beta$-P), can produce anxiolytic, sedative, and anti-convulsive effects (1, 2), and their synthetic analogs are in development as general anesthetics and for treatment of epilepsy, anxiety, depression, and other mood disorders (3, 4). These neuroactive steroids act at submicromolar concentrations as potent positive allosteric modulators (PAMs) of γ-aminobutyric acid type A receptors (GABA_AR), and at higher concentrations as direct activators in the absence of GABA (5–8). GABA_AR potentiation by steroids demonstrates structural specificity in that the orientation of a hydroxyl group at the C-3 position (Fig. 1) determines activity. Steroids with a 3α-OH, including $3\alpha5\alpha$-P and the anesthetic alphaxalone, act as PAMs, whereas their 3β-OH epimers ($3\beta5\alpha$-P and betaxalone) at higher concentrations inhibit GABA responses (9–12). This structural specificity provided early evidence that steroids might interact with specific binding sites in GABA_ARs, identification and characterization of which would prove important for the development of novel steroid-based therapeutic agents.

Functional, structural, and photolabeling studies provide evidence for the existence of multiple steroid-binding sites in $\alpha\beta\gamma$ GABA_ARs. Steroids do not bind to the GABA and benzodiazepine-binding sites at subunit interfaces in the extracellular domain or to the homologous binding sites for intravenous general anesthetics such as propofol, etomidate, and barbiturates that are located at subunit interfaces in the extracellular third of the transmembrane domain (TMD) (Fig. 1) (13, 14). Binding assays using channel blockers as well as electrophysiological assays identify multiple effects of steroids potentially mediated by distinct sites (15, 16). Intersubunit and intrasubunit steroid-binding sites near the extracellular and cytoplasmic surfaces of the TMD are predicted based upon the recently determined $\alpha1\beta3\gamma2$ GABA_AR structures (17, 18) and the locations of amino acids identified by mutational analysis as determinants for GABA_AR enhancement or direct activation. A site near the cytoplasmic end of the $\beta^+-\alpha^-$ subunit TMD interface was predicted based upon the identification of α1Gln-242 (human $\alpha1$ numbering) as a position critical for enhancement by steroids (19, 20). Consistent with this location, alphaxalone protected against the modification of cysteines substituted in the $\beta3$ M3 helix at positions contributing to this interface (21), and $3\alpha5\beta$-P, tetrahydrodeoxycorticosterone ($3\alpha5\alpha$-THDOC), and alphaxalone bind to a homologous pocket in crystallographic structures of homopentameric, chimeric receptors with GABA_AR α subunit TMDs (22–24). In $\alpha1\beta3$ GABA_ARs, there is $3\alpha5\alpha$-P inhibitable steroid photolabeling of a residue at the cytoplasmic end of βM3 in proximity to this pocket, with additional residues identified near the extracellular end of the TMD within the $\alpha1$ and $\beta3$ subunits (25).

Photoaffinity labeling with radiolabeled, photoreactive intravenous general anesthetics has allowed the identification of
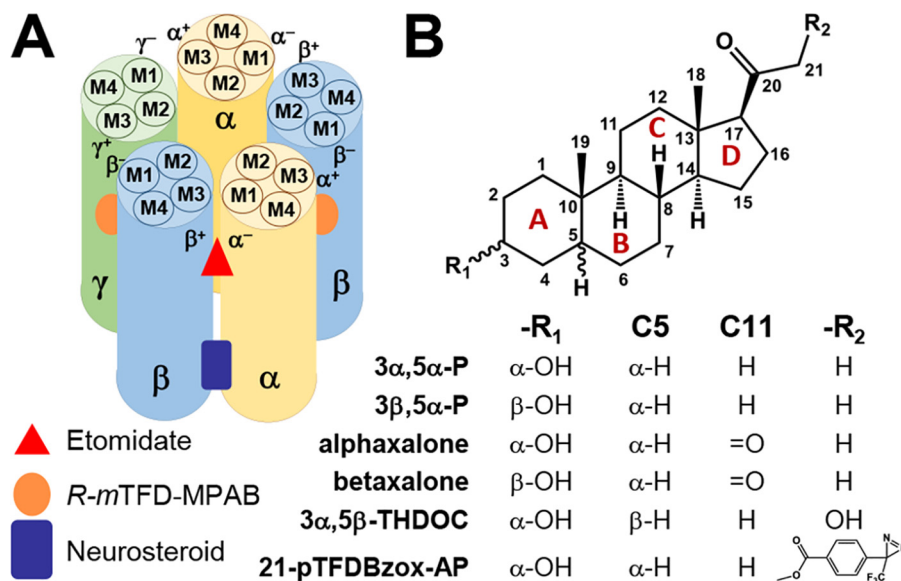
SASBMB

J. Biol. Chem. (2020) 295(33) 11495–11512 **11495**

Figure 1. Locations of general anesthetic binding sites in the TMD of an α1β3γ2 GABA_AR and structures of representative neuroactive steroids. Depicted are the four transmembrane helices in each subunit (M1–M4), the homologous binding sites for etomidate and R-mTFD-MPAB, an analog of mephobarbital, in the extracellular third of the $\beta^+ - \alpha^-$ and $\alpha^+/\gamma^+ - \beta^-$ subunit TMD interface(s), respectively, and a binding site for neuroactive steroids in the intracellular third of the $\beta^+ - \alpha^-$ interface. The binding sites for GABA are located in the extracellular domain in the $\beta^+ - \alpha^-$ subunit interfaces, and benzodiazepines bind at the homologous site in the $\alpha^+ - \gamma^-$ interface. B, steroid ring structure, with numbering of the carbons, and structures of representative neuroactive steroids that act as positive or negative GABA_AR allosteric modulators.

photolabeled amino acids for site identification and the determination of the pharmacological specificity of these sites by inhibition of photolabeling with nonradioactive anesthetics. Photolabeling with [3H]azietomidate and a mephobarbital analog, [3H]R-mTFD-MPAB, identified homologous binding sites in the α1β3γ2 GABA_AR TMD at the $\beta^+ - \alpha^-$ and $\alpha^+/\gamma^+ - \beta^-$ subunit interfaces, respectively (13, 26). Etomidate and azietomidate bind with 100-fold selectivity to the β^+ sites, R-mTFD-MPAB with 50-fold selectivity to the β^- sites, and other barbiturates and propofol derivatives bind with variable selectivity to the two classes of sites.

Here we characterize a GABA_AR steroid-binding site by use of 21-pTFDBzox-AP (21-[4-(3-(trifluoromethyl)-3H-diazirin-3-yl)benzoxy]allopregnanolone), a photoreactive steroid that acts as a potent α1β3 and α1β3γ2 GABA_AR PAM (27). Previously, we reported that [3H]21-pTFDBzox-AP primarily photoincorporated into the β3 subunit with ~80% of the subunit photolabeling inhibitable by 3α5α-P or by alphaxalone, but not by pregnenolone sulfate (PS), an inhibitory neurosteroid, or by etomidate or R-mTFD-MPAB (27). We now identify the amino acids photolabeled by [3H]21-pTFDBzox-AP, which are located at the cytoplasmic ends of the βM3 and βM4 helices and form the base of a pocket at $\beta^+ - \alpha^-$ intersubunit interface that extends up to the level of α1Gln-242 in αM1. By use of competition photolabeling with a panel of steroid GABA_AR PAMs and inhibitors, we provide a first definition of the structural determinants important for high affinity binding to this site.

Results

Positive and negative steroid GABA_AR allosteric modulators enhance [3H]muscimol binding

In equilibrium binding assays with the agonist [3H]muscimol, GABA_AR PAMs, including steroids and other general anes-

thetics, enhance binding by increasing the fraction of GABA_ARs in a desensitized state that binds [3H]muscimol with high affinity (28). 21-pTFDBzox-AP was shown previously to enhance [3H] muscimol binding to expressed α1β3 and α1β3γ2 GABA_ARs in membranes, and after purification in detergent/lipid micelles, with concentrations producing half-maximal enhancement (EC_50, 0.2-0.5 μM) similar to those for 3α5α-P, 3α5β-P, and alphaxalone (27). We extended these studies by characterizing [3H]muscimol binding to α1β3 GABA_ARs in the presence of steroids that act as GABA_AR negative allosteric modulators, inhibiting GABA responses noncompetitively: the 3β-epimers of 3α5α-P, 3α5β-P, and alphaxalone, and two 3β-sulfated steroids (PS and dehydroepiandrosterone sulfate (DHEAS)) (10, 12, 29, 30) (Fig. 2 and Table 1). The 3β-OH epimers of pregnanolone (3β5β-P) and alphaxalone (betaxalone) enhanced [3H]muscimol binding with EC_50 values of 25 and 45 μM, respectively, whereas 3β5α-P at concentrations up to 100 μM did not. PS at concentrations up to 500 μM had no effect on [3H]muscimol binding, whereas DHEAS reduced specific binding maximally by 50% (IC_50 = 10 μM). In addition, we found that (3α5α)-17-phenylandrost-16-en-3-ol (17-PA), which antagonizes steroid enhancement of GABA responses but not GABA responses (31), enhanced [3H]muscimol binding with an EC_50 of 30 μM.

Pharmacologically specific photolabeling by [3H]21-pTFDBzox-AP in the β3 subunit of α1β3 and α1β3γ2 GABA_ARs

In initial photolabeling studies, we compared [3H]21-pTFDBzox-AP photolabeling of α1β3 and α1β3γ2 GABA_ARs. After photolabeling, GABA_AR subunits were resolved by SDS-PAGE, and 3H incorporation into the subunits was characterized by fluorography (Fig. 3A). As reported previously (27), for both receptor subtypes photolabeling was most prominent in
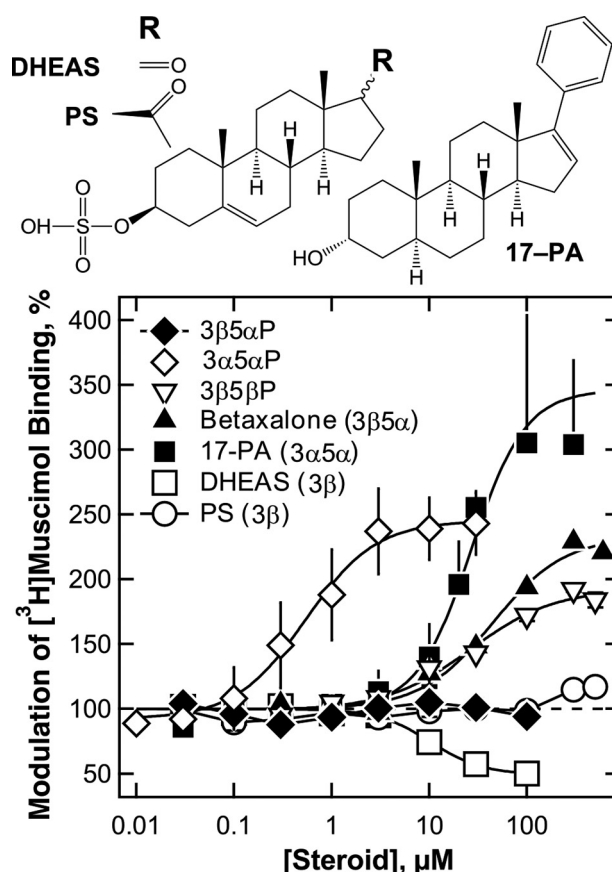
Figure 2. Modulation of GABA_AR agonist binding by steroid antagonists. The 3β-OH steroid antagonists 3β5β-P and betaxalone and the 3α-OH antagonist 17-PA enhance equilibrium binding of subsaturating concentrations of [³H]muscimol (2 nM) with efficacies similar to that seen for the PAM 3α5α-P but with lower potencies, whereas no enhancement is seen for 3β5α-P. The 3β-sulfate antagonist PS did not enhance binding, whereas DHEAS reduced specific binding maximally by 50%. The data from n independent experiments were combined and fit to determine values of EC_{50} (in μM), Hill coefficients (n_H), and maximal enhancements (B_{max}, as % control), that were: 3β5β-P (26 ± 7, 1.0 ± 0.3, 193 ± 8, n =2); betaxalone (45 ± 8, 1.2 ± 0.2, 233 ± 8, n = 2); 17-PA (29 ± 5, 1.6 ± 0.4, 352 ± 22, n = 3); 3α5α-P (EC_{50} = 0.58 ± 0.22 μM, data from Ref. 27). DHEAS (n = 4) inhibited specific binding maximally by 51 ± 2% with IC_{50} = 10.3 ± 1.6 μM and n_H = 1.6 ± 0.3.

the gel bands of 59 and 61 kDa that contain differentially glycosylated β3 subunits (13, 32), and at a lower level in the 56-kDa gel band containing the α1 and γ2 subunits. Photolabeling of the β3 subunit was inhibited by 30 μM 3α5α-P, but not by PS, etomidate, or R-mTFD-MPAB. To quantify the concentration dependence of inhibition of photolabeling by nonradioactive drugs, receptor aliquots were photolabeled with [³H]21-pTFDBzox-AP in the presence of a range of drug concentrations, with receptor subunits excised from the stained gel after SDS-PAGE and ³H incorporation into the β subunit determined by liquid scintillation counting. In a representative experiment (Fig. 3B), nonradioactive 21-pTFDBzox-AP maximally inhibited [³H]21-pTFDBzox-AP photolabeling of α1β3 and α1β3γ2 GABA_ARs to the same extent as 30 μM 3α5α-P, with IC_{50} values of 0.7 and 0.9 μM, respectively. As described under "Experimental procedures," IC_{50} values for drugs were determined by combining results from at least four independent experiments using two or more GABA_AR purifications, with data from individual experiments combined after normalization to the total specific

(*i.e.* 3α5α-P inhibitable) binding in the absence of competitor. The pooled data for inhibition by 21-pTFDBzox-AP are shown in Fig. 4.

In α1β3 and α1β3γ2 GABA_ARs, a 3α-OH substituent is a major determinant of pregnanolone affinity for this site

As a test of the pharmacological specificity of the sites identified in α1β3 and α1β3γ2 GABA_ARs by [³H]21-pTFDBzox-AP photolabeling, we compared inhibition by 3α5α-P with its antagonist 3β-OH isomer (3β5α-P) and with analogs modified at the 3-position by acetylation (3α-acetyl-5α-P), removal of the –OH (3-deoxy-5α-P), or oxidation into a ketone (3-oxo-5α-P) (Fig. 4 and Table 1). 3α5α-P inhibited photolabeling of both receptor subtypes with an IC_{50} of 0.4 μM, whereas 3β5α-P at 300 μM inhibited photolabeling of α1β3 and α1β3γ2 GABA_ARs by <10% and ~40%, respectively. At the highest concentration tested (100 μM), 3-deoxy-5α-P, which is a GABA_AR PAM (20), as well as 3α-acetyl-5α-P and 3-oxo-5α-P each inhibited photolabeling by <10%. We also determined that alphaxalone inhibited α1β3 and α1β3γ2 GABA_AR photolabeling with IC_{50} values of 5 and 2 μM, respectively, whereas for betaxalone, 50% inhibition was seen at ~200 μM (Fig. 4). Consistent with the importance of a 3α-OH for binding to this site, the sulfated 3β-OH antagonists PS and DHEAS at 100 μM each inhibited photolabeling by <10% (Table 1 and Ref. 27). In contrast to the importance of the 3α-OH, the configuration at the 5-position was not important. 3α5β-P inhibited photolabeling with an IC_{50} of 0.7 μM, similar to that for 3α5α-P, whereas 3α5α-THDOC and 3α5β-THDOC inhibited GABA_AR photolabeling with IC_{50} values of 2-3 μM (Table 1).

3α5α-P inhibits [³H]21-pTFDBzox-AP photolabeling of amino acids located at the cytoplasmic ends of the βM3 and βM4 helices that contribute to a pocket at the β⁺–α⁻ subunit interface

Based upon the similar pharmacological properties of the steroid-binding sites in α1β3 and α1β3γ2 GABA_ARs defined by [³H]21-pTFDBzox-AP photolabeling, we identified the photolabeled amino acids in α1β3 GABA_ARs, which can be expressed and purified at higher levels than α1β3γ2 GABA_ARs. β3 subunits were isolated from α1β3 GABA_ARs photolabeled on a preparative scale with [³H]21-pTFDBzox-AP (0.7 μM) in the presence of 300 μM GABA and in the absence or presence of 30 μM 3α5α-P. In five preparative photolabelings, the specific β subunit photolabeling (*i.e.* 3α5α-P inhibitable) was 320 ± 70 ³H cpm/pmol, which indicated photolabeling of 1.2 ± 0.2% of β subunits based upon the radiochemical specific activity of [³H]21-pTFDBzox-AP (21.8 Ci/mmol) and the amount of GABA_AR photolabeled. This efficiency of photolabeling was similar to that seen for GABA_AR photolabeling by a photoreactive etomidate analog (32), but ~15% the efficiency seen for [³H]R-mTFD-MPAB (33).

The photolabeled amino acids were identified by protein microsequencing of fragments beginning near the N termini of the β3M4, β3M3, and β3M1 helices that can be produced by digestion with endoproteinase Lys-C (Endo Lys-C) and resolved by reversed-phase HPLC (rpHPLC) (13, 32, 34). When

ASBMB

J. Biol. Chem. (2020) 295(33) 11495–11512 **11497**

Table 1

Comparison of potency of neuroactive steroids as modulators of [3H]muscimol binding and as inhibitors $\alpha1\beta3$ and $\alpha1\beta3\gamma2$ GABA_AR photo-labeling by [3H]21-pTFDBzoxAP

Steroid[a]	R_1 (C-3)	C5	R_2 (C-17)	[3H]Muscimol Binding[b] EC_{50}	[3H]21-pTFDBzox-AP[c] IC_{50} (n) $\alpha1\beta3$	$\alpha1\beta3\gamma2$
				μM	μM	μM
21-pTFDBzox-AP	-OH, α	α	-COCH$_2$OCOBzTFD	0.36 ± 0.06	0.21 ± 0.02 (4)	0.65 ± 0.08 (4)
3α5β-P pregnanolone	-OH, α	β	-COCH$_3$	0.62 ± 0.08	0.65 ± 0.13 (4)	0.30 ± 0.05 (4)
3α5α-P allopregnanolone	-OH, α	α	-COCH$_3$	0.58 ± 0.22	0.27 ± 0.03 (6)	0.40 ± 0.06 (6)
3β5α-P (3101-16, P3830)	-OH, β	α	-COCH$_3$	>100	>1000 (6)	470 ± 70 (2)
3β5β-P (3198-16)	-OH, β	β	-COCH$_3$	26 ± 7	>500 (4)	>300 (6)
3α-Acetyl-5α-P (P3801)	CH$_3$CO$_2$-, α	α	-COCH$_3$	>10[d]	>300 (4)	>300 (6)
3-Oxo,5α-P (P2970)	=O	α	-COCH$_3$	>10[d]	>300 (4)	>300 (2)
3-Deoxy-5α-P (P4230)	-H	α	-COCH$_3$	1[e]	>300 (4)	>300 (2)
Alphaxalone (11-oxo)	-OH, α	α	-COCH$_3$	0.71 ± 0.15	4.6 ± 0.7 (4)	2.4 ± 0.5 (4)
Betaxalone (11-oxo) (3093-16)	-OH, β	α	-COCH$_3$	45 ± 8	175 ± 25 n_H = 0.5 ± 0.1 (6)	200 ± 50 (2)
3α5α-THDOC (P2560)	-OH, α	α	-COCH$_2$OH	1.0 ± 0.15	2.1 ± 0.3 (4)	ND
3α5β-THDOC (3167-16)	-OH, α	β	-COCH$_2$OH	3[e]	3.3 ± 0.5 (4)	2.9 ± 0.5 (4)
DHEAS (5-ene)	SO$_4$-, β	–	=O	IC_{50} = 10 ± 2	>300 (4)	>300 (4)
PS (5-ene)	SO$_4$-, β	–	-COCH$_3$	>300	>300 (4)	>300 (6)

[a] Catalog numbers are indicated for steroids from Research Plus (xxxx-16) and Steraloids (P-xxxx).
[b] EC_{50} (±S.E.) values for steroid modulation of 2 nM [3H]muscimol binding to $\alpha1\beta3$ GABA_AR in membranes, from Fig. 2 and Ref. 27.
[c] IC_{50} (±S.E.) values, the total drug concentrations resulting in 50% inhibition of photolabeling of GABA_AR purified in detergent/lipid, were determined as described under "Experimental procedures," from Fig. 4 and Ref. 27. n, number of experiments.
[d] EC_{50} values for enhancement of [3H]flunitrazepam binding to rat brain membranes (51).
[e] EC_{50} values for enhancement of GABA responses of expressed $\alpha1\beta2\gamma2$ GABA_AR (12, 20).

aliquots of the β subunit Endo Lys-C digests were sequenced, peaks of ^{3}H release were seen in cycles 3/4 and 6/7 that were inhibitable by 3α5α-P (Fig. 5A). When the digests were fractionated by rpHPLC (Fig. 5B), the peak of ^{3}H was recovered in a fraction that contained an unlabeled fragment beginning at β3Ala-280 near the N terminus of βM3, with the unlabeled fragment beginning at β3Ile-412 before the N terminus of βM4 eluting one fraction earlier. Additional ^{3}H-containing adducts eluted in the more hydrophobic fractions that contain the unlabeled fragment beginning at β3Arg-216 at the N terminus of βM1 that extends through βM2.

Protein sequencing protocols were designed to allow identification of photolabeled amino acids even if the incorporation of the hydrophobic steroid caused the ^{3}H-labeled fragment to elute in more hydrophobic HPLC gradient fractions than the unlabeled fragment directly identifiable by PTH-derivative analysis. When 50% of the fraction containing the peak of ^{3}H was sequenced, there were peaks of ^{3}H release in cycles 3-4 and 6-7 of Edman degradation that were reduced by 90% by 3α5α-P (Fig. 5C), as seen when the total digest was sequenced. There were no additional peaks of ^{3}H release above background in 30 cycles of Edman degradation (not shown). To determine whether the peaks of ^{3}H release originated from labeling in βM3 or βM4, we took advantage of the presence of β3Pro-415 in cycle 4 of Edman degradation of the βM4 fragment and the lack of a proline at that cycle in the βM3 or βM1 fragment. For the remaining 50% of the fraction, sequencing was interrupted at cycle 4 for treatment with o-pthalaldehyde (OPA) to prevent further sequencing of fragments not containing a proline at that cycle (35, 36). After treatment with OPA in cycle 4, the

^{3}H releases in cycles 4, 6, and 7 were preserved, whereas sequencing of the M3 fragment was reduced by >95% (Fig. 5C). Thus, these ^{3}H releases did not originate from the βM3 fragment. Rather, the results were consistent with 3α5α-P inhibitable photolabeling of β3Pro-415 (cycle 4), β3Leu-417, and β3Thr-418 in the fragment beginning at β3Ile-412 before the N terminus of βM4. The ^{3}H release in cycle 3, although not tested by the use of OPA in cycle 4, indicated likely labeling of β3Ile-414. Based upon sequencing nine samples from five independent photolabeling experiments, β3Ile-414 and β3Leu-417 were photolabeled at 55 ± 26 and 155 ± 55 cpm/pmol, respectively, ~90% inhibitable by 3α5α-P (Table 2). Because of uncertainties in calculating photolabeling efficiency for the second of two successive photolabeled amino acids, similar calculations were not made for β3Pro-415 and β3Thr-418.

Photolabeling of β3Arg-309 at the C terminus of βM3 was identified by sequencing the broad peak of ^{3}H that co-eluted with the unlabeled βM1 fragment (Fig. 6). A peak of 3α5α-P inhibitable ^{3}H release was seen in cycle 30, in addition to the peaks of ^{3}H release in cycles 3/4 and 6/7 attributable to labeling within the βM4 fragment and a peak in cycle 19 not reproduced in other experiments (Fig. 6A). The ^{3}H release in cycle 30 did not result from labeling in βM1, because for a sample sequenced with OPA treatment at cycle 13, the cycle containing β3Pro-228 in βM1, sequencing of the βM1 fragment persisted after treatment but no release of ^{3}H was seen in cycle 30 (not shown). This suggested that the labeled βM3 fragment, similar to the labeled βM4 fragment, eluted in more hydrophobic rpHPLC fractions than the unlabeled fragment, with the ^{3}H release in cycle 30 resulting from
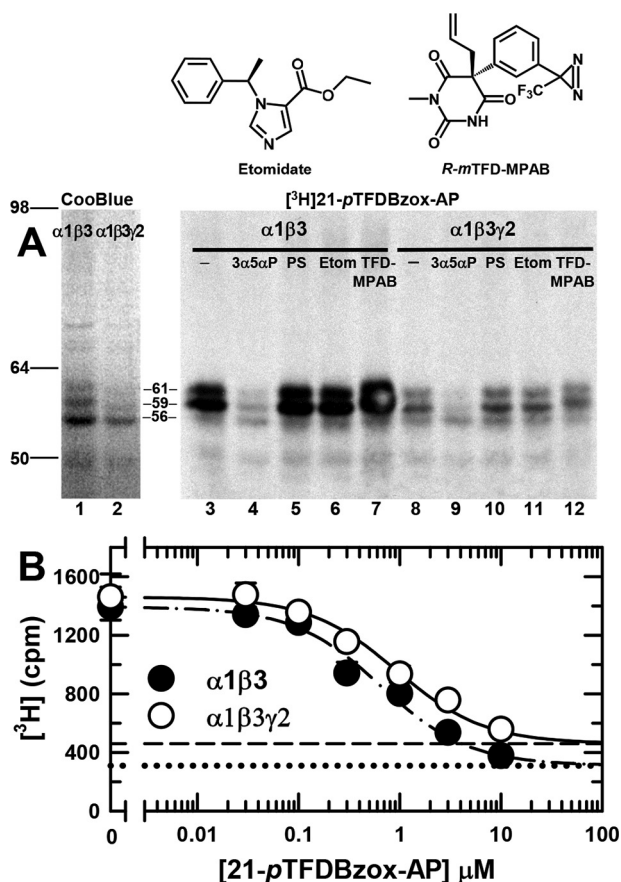
Figure 3. 3α5α-P and 21-*p*TFDBzox-AP, but not PS, inhibit [³H]21-*p*TFDBzox-AP (0.5 μM) photolabeling of α1β3 and α1β3γ2 GABA_ARs. GABA_AR aliquots were equilibrated in the presence of 300 μM GABA, in the absence or presence of 3α5α-P, PS, etomidate, or *R*-*m*TFD-MPAB. After photolabeling, receptor subunits were resolved by SDS-PAGE and ³H incorporation was determined by fluorography (*A*) or by liquid scintillation counting of excised subunits (*B*). *A*, lanes *1* and *2* are representative Coomassie Blue-stained gel lanes from the gel used for fluorography. The fluorogram (*lanes 3–12*) compares ³H incorporation into α1β3 (*lanes 3–7*) and α1β3γ (*lanes 8–12*) GABA_ARs photolabeled in the presence of GABA (*lanes 3* and *8*), or in the presence of GABA and 30 μM 3α5α-P (*lanes 4* and *9*), 100 μM PS (*lanes 5* and *10*), 300 μM etomidate (*lanes 6* and *11*), or 60 μM *R*-*m*TFD-MPAB (*lanes 7* and *12*). Indicated on the *left* of lane *1* are the mobilities of the molecular mass markers (98, 64, and 58 kDa) and between *lanes 2* and *3* the calculated mobilities of the GABA_AR subunit bands (α1, 56 kDa; β3, 59/61 kDa; with the γ2 subunit distributed diffusely in this region). *B*, in separate experiments, α1β3 and α1β3γ2 GABA_ARs were equilibrated with [³H]21-*p*TFDBzoz-AP, GABA, and increasing concentrations of nonradioactive 21-*p*TFDBzox-AP or 30 μM 3α5α-P. After photolabeling, receptor subunits were separated by SDS-PAGE, and ³H incorporation was determined in the excised gel bands. For each receptor, two experiments were run in parallel, and the plotted data are the ³H incorporation in the β subunit (59/61 kDa) gel bands (mean ± ½ range). The curves are the fits of the data to a single site model, with B_{ns} fixed at the observed photoincorporation in the presence of 30 μM 3α5α-P (α1β3 (*dotted line*), 310 ± 30 cpm; α1β3γ2 (*dashed line*), 460 ± 16 cpm). For α1β3 and α1β3γ2 GABA_ARs, the IC_50 values were 0.65 ± 0.1 μM (R^2 = 0.95) and 0.92 ± 0.16 μM (R^2 = 0.94), respectively. In the α1 (56 kDa) gel bands, control and nonspecific ³H incorporation (in cpm) were 370 ± 40/140 ± 10 (α1β3) and 430 ± 60/240 ± 13 (α1β3γ2).

photolabeling of β3Arg-309. To test this, we generated a fragment beginning at β3Gly-287 in βM3 by use of cyanogen bromide to cleave at the C terminus of β3Met-287 (as well as other methionines in the sample on the sequencing filter). When this fragment was sequenced, there was a peak of 3α5α-P inhibitable ³H release in cycle 23 consistent with photolabeling of β3Arg-309 (Fig. *6B*). Based upon results
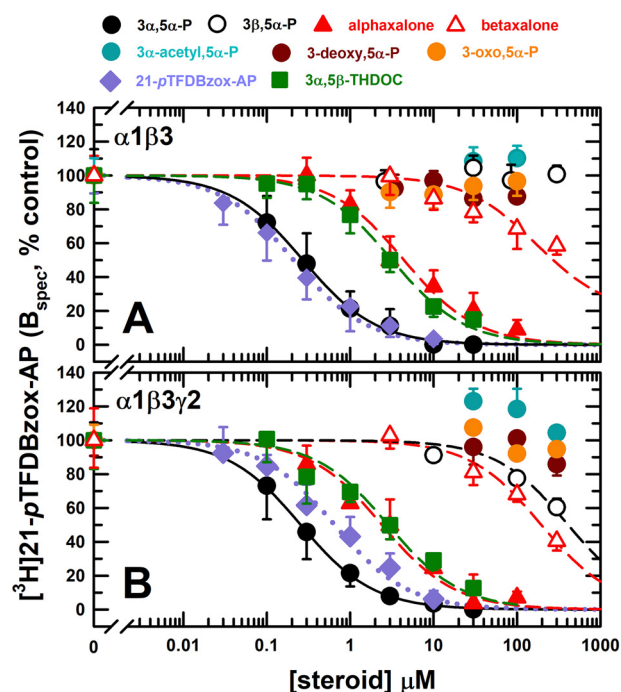

Figure 4. A free 3α-OH is a major determinant of high affinity binding of pregnane steroids to the [³H]21-*p*TFDBzox-AP GABA_AR site. α1β3 GABA_ARs (*A*) or α1β3γ2 GABA_ARs (*B*) were photolabeled in the presence of GABA and varying concentrations of pregnane steroids containing a 3α-OH (3α5α-P, 3α5β-THDOC, alphaxalone, 21-*p*TFDBzox-AP), a 3β-OH (3β5α-P, betaxalone), or lacking a free 3-OH (3α-acetyl-5α-P, 3-deoxy-5α-P, 3-oxo-5α-P). After SDS-PAGE, covalent incorporation of ³H in the β subunit was determined by liquid scintillation counting. For each independent experiment, nonspecific photolabeling (B_{ns}) was determined in the presence of 30 μM 3α5α-P, and specific binding was normalized to the ³H cpm incorporated specifically in the control condition ($B_0 - B_{ns}$). The plotted data are the averages (± S.D.) from the independent experiments. As described under "Experimental procedures," the pooled data from the independent experiments were fit to Equation 2. Drug structures, parameters for the fits, and the number of independent experiments are tabulated in Table 1. The curves are plotted for fits to n_H =1, which were favored by *F*-test comparison over fits with variable n_H, with the exception of betaxalone (α1β3, n_H = 0.5 ± 0.1). Based upon an *F*-test comparison of fits of the data for α1β3 and α1β3γ2 GABA_ARs to the same (null hypothesis) or separate IC_50 values, a common fit was favored for 3α5α-P (p = 0.7, *F*(DFn,DFd) = 0.22 (1,112)) and 3α5β-THDOC (p = 0.6, *F*(DFn,DFd) = 0.24(1,63)). Separate fits were favored for 21-*p*TFDBzox-AP (p < 0.0001, *F*(DFn,DFd) = 35.9(1,94)), 3α5β-P (p = 0.002, *F*(DFn,DFd) = 10.4 (1,62)), and alphaxalone (p = 0.01, *F*(DFn,DFd) = 6.7(1,62)).

from 4 independent photolabeling experiments, β3Arg-309 was photolabeled at ∼25% the efficiency as compared with β3Leu-417 (Table 2).

[³H]21-*p*TFDBzoxy-AP photolabeling in GABA_AR α subunit

Because β subunit photolabeling dominated over that in α and the gel band containing α subunit also contains β subunit at a low level (13), it was difficult to use our protocols to determine whether α subunit residues were photolabeled at low efficiency. Nonetheless, we searched in particular for 3α5α-P inhibitable photolabeling in αM4 at αAsn-408, which is an intrasubunit residue near the extracellular end of TMD that is a sensitivity determinant for steroid enhancement (19) and that was photolabeled by an allopregnanolone derivative with a photoreactive group at C-21 (25). The latter also photolabeled β3Gly-308 or β3Arg-309 in the β⁺−α⁻ steroid site. In parallel with the β subunit studies, we fractionated α subunit Endo Lys-
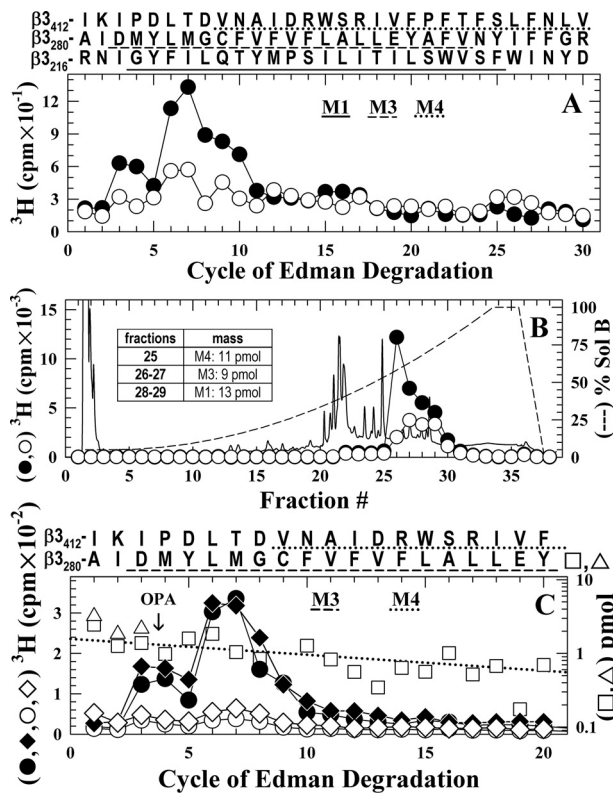
Figure 5. 3α5α-P inhibits [³H]21-*p*TFDBzox-AP photolabeling of β3Ile-414, β3Pro-415, β3Leu-417, and β3Thr-418 near the N terminus of βM4. α1β3 GABA$_A$Rs were photolabeled on a preparative scale in the presence of 300 μM GABA in the absence or presence of 30 μM 3α5α-P. GABA$_A$R β subunits were isolated by SDS-PAGE and digested with Endo Lys-C. *A*, when digested, aliquots (10%) were sequenced without further purification, there were peaks of ³H release in cycles 3/4 and 6/7 for the sample photolabeled in the absence (●) but not the presence (○) of 3α5α-P. Shown above are the sequences of the β3 subunit fragments produced by Endo Lys-C digestion that contain transmembrane helices (M1–M2, M3, and M4). *B*, ³H elution profiles when the Endo Lys-C digests were fractionated by rpHPLC, determined by counting 10% of each fraction. *Inset,* Edman degradation determination of the masses (I_0) of β subunit fragments eluting in rpHPLC fractions 25 (βM4), 26/27 (βM3), and 28-29 (βM1). *C*, ³H released during sequence analysis of the peak of ³H (rpHPLC fraction 26) from receptors photolabeled in the absence (●, ♦) and presence (○, ◇) of 3α5α-P and released PTH-derivatives (□, △) in the absence of 3α5α-P. Equal aliquots were sequenced normally (●, ○, □) or with sequencing interrupted at cycle 4 for treatment with OPA (♦, ◇, △) to prevent further sequencing of the βM3 fragment not containing a proline at that cycle. In the absence of OPA, the PTH-derivatives from the β3Ala-280 fragment (□, I_0 = 1.6 pmol) were detected for 20 cycles of Edman degradation. OPA treatment (△) prevented further sequencing of that fragment, but did not alter the pattern of ³H release, with peaks in cycles 3/4 and 6/7 without (●) or with (♦) OPA. The persistence of ³H release in cycles 4, 6, and 7 after OPA treatment was consistent with photolabeling of β3Pro-415, β3Leu-417, and β3Thr-418. This photolabeling was inhibitable by 3α5α-P, because the peaks of ³H release were reduced by 90% (without (○) or with (◇) OPA) when fraction 26 was sequenced from receptors photolabeled in the presence of 3α5α-P.

C digests by rpHPLC and found a ³H distribution similar to that for β subunit digests shown in Fig. 5*B*. We sequenced fractions 24-27 that would contain the unlabeled and labeled fragments beginning at α1Ileu-392, with OPA treatment in cycle 10 of Edman degradation (α1Pro-401) to associate ³H release beyond cycle 11 (α1Leu-402) with αM4. When the α1Ile-392 fragment (I_0 = 6 pmol) was sequenced for 25 cycles, no peaks of ³H release were detected above background after cycle 11. Any photolabeling of α1Asn-408, or residues nearby in the primary structure, if it occurred, would be at less than 10% the efficiency of photolabeling of β3Leu-417.

Table 2

Pharmacological specificity of [³H]21-*p*TFDBzox-AP photoincorporation into β3Ile-414, β3Leu-417, and β3Arg-309 in the α1β3 GABA$_A$R in the presence of GABA

The efficiency of photolabeling of a residue (in cpm/pmol of PTH-derivative) was calculated using Equation 4 ("Experimental procedures"). The data for the control condition are presented as mean (± S.D.) from 4 (β3Arg-309) or 5 (β3Ile-414, β3Leu-417) independent photolabeling experiments with the number (*n*) of sequenced samples. Samples from GABA$_A$Rs photolabeled in the absence (control) or presence of 30 μM 3α5α-P were sequenced in parallel. For each pair the percent inhibition at that residue was calculated from the ratio of calculated photolabeling efficiencies, with the mean (± S.D.) for all samples tabulated.

	Control	*n*	+3α5α-P inhibition
	cpm/pmol		*%*
β3Ile414	55 ± 26	9	92 ± 7
β3Leu417	155 ± 55	9	88 ± 6
β3Arg309	37 ± 22	5	90 ± 7

Locations of photolabeled residues in α1β3γ2 GABA$_A$R structure

In Fig. 7 we highlight the positions of four photolabeled residues (β3Pro-415, β3Leu-417, β3Thr-418, and β3Arg-309) in a structure recently solved by cryo-EM (18) of α1β3γ2 GABA$_A$Rs (Protein Data Base 6I53) purified from the same GABA$_A$R-expressing HEK 293T cell line used for our purifications. Most of the 116 amino acids comprising the β3 cytoplasmic domain between the M3 and M4 helices are not defined in this structure, which resolves amino acids beginning with β3Pro-415 and locates β3Val-420 at the cytoplasmic end of the βM4 helix. In this structure, β3Pro-415–β3Asp-419 form a turn at the cytoplasmic end of βM4, with the photolabeled residues (β3Pro-415, β3Leu-417, β3Thr-418, and β3-Arg-309 at the cytoplasmic end of βM3) contributing to the base of a pocket at the β$^+$−α$^-$ subunit interface (Fig. 7, *B* and *C*) that extends between βM3 and αM1 up to the level of α1Gln-242, the amino acid in αM1 identified by mutational analysis as a major sensitivity determinant for many steroid PAMs (19), including 21-*p*TFDBzox-AP (27). This pocket is homologous to the intersubunit cleft identified as a binding site for 3α-OH steroid PAMs in crystal structures of homomeric, chimeric receptors containing GABA$_A$R α subunit TMDs (22–24). Based upon computational docking using CDocker, 21-*p*TFDBzoxy-AP can be readily accommodated within this intersubunit pocket in the α1β3γ2 GABA$_A$R β$^+$−α$^-$ subunit interface, with the lowest energy solutions adopting an orientation with the 3α-OH in proximity to α1Gln-242 and with the reactive diazirine in proximity to the photolabeled residues (Fig. 7*C*).

Anesthetic, anticonvulsant, and anxiolytic 3α-OH steroids bind to this site

By use of competition photolabeling, we established that this site binds with high affinity a structurally diverse group of 3α-OH pregnane GABA$_A$R PAMs that have a wide range of pharmacological activities *in vivo* (Fig. 8*A* and Table 3). Org20599, an amino steroid anesthetic containing a 2β-morpholino-substituent to enhance water solubility (37), inhibited photolabeling with IC$_{50}$ = 0.2 μM. Substitutions at the 3β- and 17β-positions that improve bioavailability were well tolerated. Thus, GABA$_A$R PAMs that act *in vivo* as an anticonvulsant (ganaxolone (38)), an anti-depressant (SAGE-217 (39)), or a sedative/hypnotic (CCD-3693 (40)) each inhibited photolabeling with
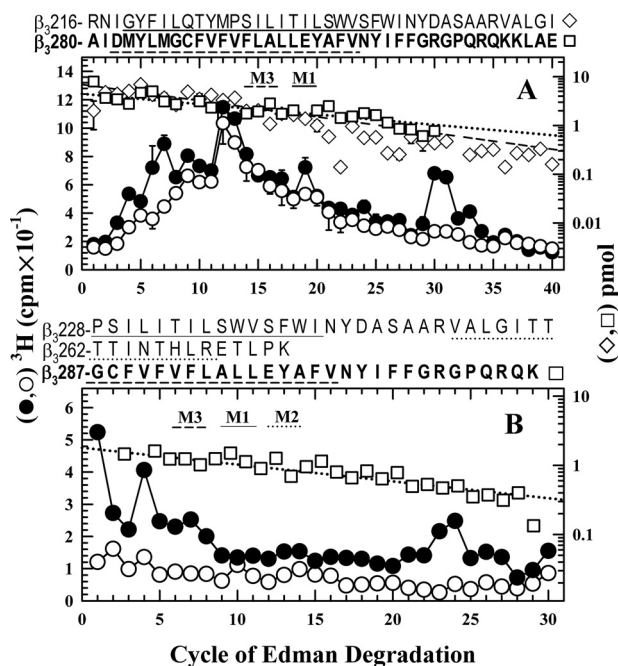
β3216- RN IGYF I LQTYMPS I L I T I LSWVSFWINYDASAARVALGI ◇
β3280- A I DMYLMGCFVFVFLALLEYAFVNY I FFGRGPQRQKKLAE □

β3228-PS I L I T I LSWVSFWINYDASAARVALGITT
β3262-TT INTHLRETLPK
β3287-GCFVFVFLALLEYAFVNY I FFGRGPQRQK □

Figure 6. 3α5α-P inhibits [³H]21-*p*TFDBzox-AP photolabeling of β3Arg-309 near the cytoplasmic end of M3. *A*, ³H (●, ○) and PTH-derivatives (◇) released during sequence analysis of rpHPLC fractions 28-30 (from Fig. 5*B*) from receptors photolabeled in the absence (●, ◇) and presence (○) of 3α5α-P. Samples were sequenced in duplicate, and the ³H release is plotted as mean cpm (±½ range). The primary sequence began at β3Arg-216 at the N terminus of βM1 (◇, I₀ = 6 pmol) with the β3Ala-280 fragment present at 10% of that level (not shown). Also plotted are the PTH-derivatives released (□) for the total amount of the β3Ala-280 fragment sequenced in fractions 26-30 (I₀ = 9 pmol). The peak of 3α5αP-inhibitable ³H release in cycles 30/31 of Edman degradation was not seen when fractions 26 or 27 were sequenced (not shown). If the increased hydrophobicity of the photolabeled β3Ala-280 fragment shifted its elution to more hydrophobic fractions than the unlabeled fragment, which eluted in fractions 26-27, the peak of ³H release in cycle 30 would result from 3α5α-P inhibitable photolabeling of β3Arg-309 near the C terminus of βM3. The following experiment tested this hypothesis. *B*, ³H (●, ○) and PTH-derivatives (□) released during sequence analysis of a β3 subunit fragment beginning at β3Gly-287 confirms 3α5α-P inhibitable photolabeling of β3Arg-309. From an independent preparative photolabeling of GABA$_A$Rs in the absence (●, □) and presence (○) of 3α5α-P, rpHPLC fractions 25-29 were pooled for sequencing from Endo Lys-C digests of β subunits. Samples were first sequenced for 20 cycles with OPA treatment at cycle 4 (not shown), then sequencing was interrupted for treatment with cyanogen bromide to cleave at methionines (see "Experimental procedures"). After treatment, the fragment beginning at β3Gly-287 (□, I₀ = 1.8 pmol) was sequenced along with fragments beginning at β3Pro-228 in βM1 and β3Thr-262 in βM2. The peak of ³H release in cycle 23 seen for photolabeling in the absence (●) but not in the presence (○) of 3α5α-P was consistent with photolabeling of β3Arg-309 at 30 cpm/pmol. This efficiency was the same as that calculated for β3Arg-309 photolabeling based upon the peak of ³H release seen in cycle 30 when a parallel aliquot of the pool of fraction 25–29 was directly sequenced for 35 cycles (not shown). If photolabeling of β3Asp-245 in βM1 was the source of ³H release in cycle 30 (*A*), the peak of ³H release would have shifted to cycle 18 when sequencing the β3Pro-228 fragment. The identity of the photolabeled amino acid associated with the peak of ³H release in cycle 4 is uncertain. The absence of peaks of ³H release in cycles 11 and 16 of *A* rules out labeling of βVal-290 in βM3 or βLeu-232 in βM1; β3Asn-265 may be photolabeled at ~10% the efficiency of β3Leu-417.

IC$_{50}$ < 1 μM, and for UCI-50027, active orally as an anxiolytic (41), the IC$_{50}$ was 10 μM. 3β-CH$_3$OCH$_2$-3α,5α-THDOC (42) (IC$_{50}$ = 2 μM) was equipotent with 3α,5α-THDOC as an inhibitor. Each of these compounds inhibited photolabeling maximally to the same extent as 30 μM 3α5α-P, with the exception of ganaxolone, which inhibited maximally by only 71 ± 2%.

Substitutents at C-17 in the steroid D ring are important determinants of binding affinity

In contrast to the high affinity binding of 3α5α-P and 3α5β-P, the presence of a hydroxyl group at the C-20 position in place of the carbonyl resulted in loss of binding. 5α-Pregnan-3α,20α-diol or 5β-pregnan-3α,20β-diol at 300 μM inhibited photolabeling by <10%, although they act as GABA$_A$R PAMs with potencies similar to 3α5α-P (30, 43) (Fig. 8*A*). The presence of the −OH at C-20 caused the loss of binding, because 5β-pregnan-3α-ol (3α5β-P-20-deoxy), with hydrogens at C-20, bound with high affinity (IC$_{50}$ = 4 μM), as did 5α-androstan-3α-ol (3α5α-A, IC$_{50}$ = 9 μM)) without any C-17 substituent (Fig. 8*B* and Table 4). Similar to the loss of binding associated with an −OH at C-20, the presence of an −OH or a carbonyl at C-17 also reduced binding affinity. At 300 μM, androsterone (3α5α-A-17-one), a potent GABA$_A$R PAM (30, 44), inhibited photolabeling by only ~40%, and 5α-androstan-3α,17α-diol (3α5α-A-17α-ol) inhibited photolabeling by <10%. In contrast to the steroid PAMs that bound with high affinity to this site and inhibited photolabeling with a Hill coefficient (n_H) close to 1, 3α5α-A-17-one inhibited photolabeling with n_H less than 0.5 (IC$_{50}$ = 700 ± 390 μM, n_H = 0.32 ± 0.05). The 3α-OH androstene antagonist 17-phenyl-(3α,5α)-androsten-16-en-3-ol (17-PA) was more potent than 3α5α-A-17-one as an inhibitor for photolabeling, with IC$_{50}$ = 85 ± 13 μM, n_H = 0.33 ± 0.03.

The binding of C-11 substituted pregnanolones

As the carbonyl at C-11 in alphaxalone reduced its IC$_{50}$ value by 20-fold compared with 3α5α-P (Table 1), we used competition photolabeling to determine the effects of other C-11 substituents on binding to this site (Fig. 9 and Table 5). As seen for the C-11 carbonyl in alphaxalone, the affinity for the 5β analog of alphaxalone (renanolone, IC$_{50}$ =10 μM) was 20-fold weaker than that for 3α5β-P. Substitution of an 11β-OH further reduced potency by 20-fold (3α5β-P-11β-ol, IC$_{50}$ ∼ 200 μM). In contrast, high affinity binding was retained in the presence at C-11 of either the small azi-group (11-Azi-AP, IC$_{50}$ = 0.4 μM) or the bulky azidotetrafluorophenyl-group (11-F4N3Bzoxy-AP, IC$_{50}$ = 0.1 μM) in two recently introduced photoreactive 3α5α-P derivatives that act as potent GABA$_A$R PAMs and general anesthetics (45).

Simultaneous binding with nonsteroidal GABA$_A$R PAMs at the etomidate site

We used competition photolabeling to determine whether PAMs of large size that bind to the etomidate site near the extracellular end of the TMD β⁺−α⁻ subunit interface would inhibit [³H]21-*p*TFDBzox-AP photolabeling of α1β3 GABA$_A$Rs, whether by steric overlap or by negative allosteric interaction. Less than 10% inhibition was seen at the highest concentrations tested for propofol (300 μM, molecular volume, 191 Å³), etomidate (300 μM, volume 208 Å³), or TG-41 (10 μM, ethyl 2-(4-bromophenyl)-1-(2,4-dichlorophenyl)-1*H*-4-imidazolecarboxylate (46), volume 323 Å³), which were tested at 40-, 150-, and 500-fold higher than their IC$_{50}$ values for inhibition of [³H] azietomidate photolabeling (26).
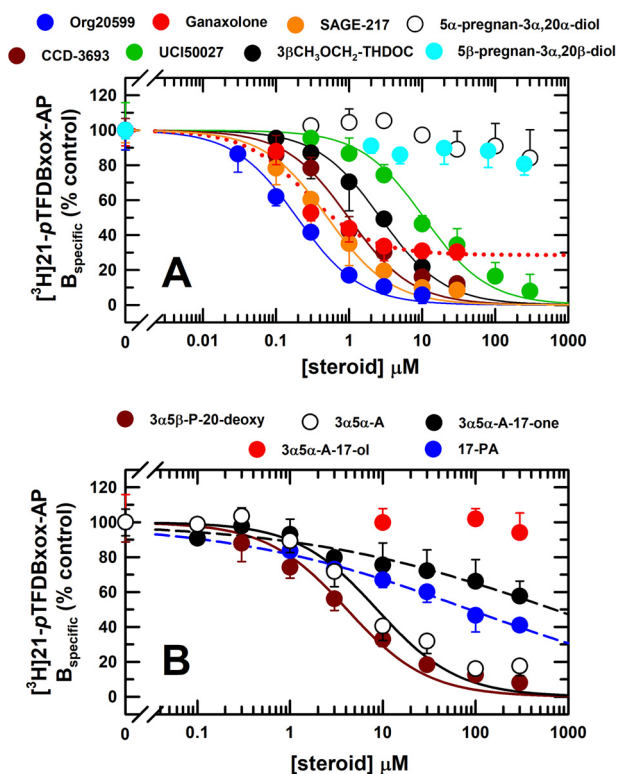
Figure 7. Location of the [³H]21*p*-TFDBzox-AP labeled residues in the cytoplasmic domain of the α1β3γ2L GABA_AR (PDB 6I53). *A*, a partial alignment of the human α1, β3, and γ2L GABA_AR subunits' M3 and M4 helices (denoted by *heavy lines*) with cytoplasmic extensions, with amino acid numbering of the subunits after signal sequence cleavage. *Asterisks* (*) denote conserved residues in the alignments, and *dashed lines* designate residues resolved in the PDB 6I53 GABA_AR structure (18). Residues photolabeled by [³H]21*p*-TFDBzox-AP are color-coded: β3Arg-309 (*crimson*); β3Ile-414 (*red*); β3Pro-415 (*orange*); β3Leu-417 (*lime green*); and β3Thr-418 (*magenta*). *B* and *C*, images of the PDB 6I53 structure with *horizontal lines* approximating membrane-aqueous interfaces. In *B*, α-helices are *cylinders* and β-sheets are *ribbons*. Binding sites for GABA (*green*, overlaid from PDB 6HUJ), etomidate (*red*, docked), and αTHDOC (*blue*, docked) are included. *C*, an expanded view of the TMD at a β⁺–α⁻ interface with the [³H]21*p*-TFDBzox-AP labeled residues (β3Arg-309, β3Pro-415, β3Leu-417, and β3Thr-418) highlighted. These residues are shown as Connolly surfaces, as are the others that contribute to an intersubunit pocket extending to αGln-242 (*purple*), a residue identified by mutational analysis as a steroid sensitivity determinant (19). 21*p*-TFDBzox-AP is in stick format, docked in this pocket in its lowest energy orientation with a transparent Connolly surface of the 9 lowest energy solutions. In this orientation, the photoreactive diazirine is within 5 Å of β3Arg-309, β3Leu-417, and β3Thr-418, and the 3α-OH is within 5 Å of αGln-242 and 3 Å of αTrp-246, a residue also identified by mutational analysis as a steroid sensitivity determinant (20). Also shown is the etomidate-binding site in the β⁺–α⁻ interface near the extracellular end of the TMD, defined by the residues photolabeled by etomidate analogs and by mutational analysis (β3Met-286, β3Val-290, α1Leu-232, and α1Met-236 (32, 69)) and a docked etomidate (in stick figure).

We also tested ivermectin (volume 880 Å³), a nonanesthetic activator and PAM of GABA_ARs and other pentameric ligand-gated ion channels (47) that binds in a homomeric, invertebrate glutamate-gated chloride channel (Glu-Cl) to an intersubunit site (48) homologous to the etomidate and *R-m*TFD-MPAB sites in α1β3 or α1β3γ2 GABA_ARs. In α1β2γ2 GABA_ARs, however, mutational analysis indicate that ivermectin interacts nonequivalently with these sites, with the γ⁺–β⁻ site most important for activation (49). We found that 100 μM ivermectin inhibited [³H]21-*p*TFDBzox-AP photolabeling of α1β3 or α1β3γ2 GABA_ARs by <10% (Fig. 10). In contrast, ivermectin potently inhibited photolabeling by [³H]*R-m*TFD-MPAB (IC_{50} = 0.02 ± 0.005 μM, n_H = 0.6 ± 0.1) and inhibited [³H]azietomidate

photolabeling at higher concentrations (IC_{50} = 6.4 ± 1.0 μM) (Fig. 10). Thus, ivermectin at 100 μM fully occupies those sites without inhibiting [³H]21-*p*TFDBzox-AP photolabeling, and consistent with the functional studies, ivermectin binds with higher affinity to the α⁺/γ⁺–β⁻ sites than to the β⁺–α⁻ sites. Furthermore, the concentration dependence of inhibition of [³H]*R-m*TFD-MPAB photolabeling (n_H = 0.6) established that ivermectin binds nonequivalently to the α⁺–β⁻ and γ⁺–β⁻ sites in the presence of GABA. This is not the case for *R-m*TFD-MPAB, but it is for other GABA_AR PAMs including the anesthetic *p*-benzoyl-propofol and the sedative/anticonvulsant loreclezole (26). Based upon a fit of the inhibition data to a two-site model, ivermectin binds to the β⁻ sites with IC_{50} values of 3.1 ± 1.1 and

Figure 8. Structural determinants for binding of 3α-OH pregnanes and androstanes to the [³H]21p-TFDBzox-AP site in α1β3 GABA$_A$Rs. GABA$_A$Rs were photolabeled in the presence of GABA and the indicated concentrations of a panel of GABA$_A$R PAMs or the androstene antagonist 17-PA. Covalent incorporation of ³H was determined by liquid scintillation counting of β3 subunits isolated by SDS-PAGE, and data from independent experiments were normalized and combined as described under "Experimental procedures" and Fig. 4. The plotted data are the mean ± S.D. from the independent experiments. For each steroid tested, the chemical structure, the parameters (IC$_{50}$, n_H) determined from the concentration dependence of inhibition, and the number of independent experiments are presented in Tables 3 and 4. *A*, substitutions at the 2β- (Org-20599) and 3β- (ganaxolone, SAGE-217, CCD-3693, UCI-50027) positions are well tolerated, as is the presence at C-19 of an -H (SAGE-217, CCD-3693) rather than –CH$_3$. Pregnanes with a carbonyl at C-20 bind with high affinity, but those with an –OH do not. With the exception of ganaxolone (B_{ns} = 28.6 ± 1.6%), curves were calculated from fits with B_{ns} = 0 and n_H = 1. *B*, substituents at steroid carbon 17 (C-17) are a major determinant of binding affinity. 5α-Androstan-3α-ol (3α5α-A), with hydrogens at C-17, and 3α5β-P-20-deoxy, with a 17β-ethyl substituent, bind to this site, but 3α5α-A17α-ol does not. Inhibition curves were calculated from fits with B_{ns} = 0 and variable n_H for 5αA3α-ol,17-one (IC$_{50}$ = 700 ± 390 μM, n_H = 0.32 ± 0.05, R^2 = 0.72) and 17-PA (IC$_{50}$ = 85 ± 13 μM, n_H = 0.33 ± 0.02, R^2 = 0.95). Inhibition by 3α5α-A-17-one was fit equally well to Equation 2 with variable B_{ns} and n_H = 1 (B_{ns} = 63 ± 3%, IC$_{50}$ = 5 ± 2 μM, R^2 = 0.71) but not for inhibition by 17-PA (R^2 = 0.47).

150 ± 65 nM. Further studies would be required to determine whether it is the α$^+$–β$^-$ or γ$^+$–β$^-$ site that binds with highest affinity.

Discussion

In this report we show that a novel photoreactive steroid, [³H]21-*p*TFDBzoxy-AP, binds with high affinity to a site in the TMD of heteromeric GABA$_A$Rs at the cytoplasmic end of the β$^+$–α$^-$ subunit interface, and we use a photolabeling inhibition assay to provide a first definition of the structure-affinity relationships for a GABA$_A$R steroid-binding site. In α1β3 and α1β3γ2 GABA$_A$Rs, pharmacologically specific [³H]21-*p*TFD-Bzoxy-AP photolabeling was primarily within the β subunit,
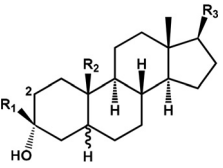
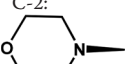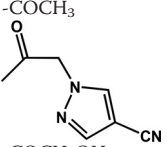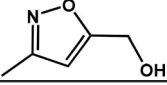with the photolabeled amino acids located in the GABA$_A$R structure near the cytoplasmic ends of the βM4 (β3Pro-415, β3Leu-417, and β3Thr-418) and βM3 (β3Arg-309) helices that contribute to the base of a pocket at the β$^+$–α$^-$ subunit interface. This binding site extends upward to the level of α1Gln-242, a position identified by mutational analysis as a major determinant for steroid enhancement of GABA responses. Many 3α-OH pregnane and androstane GABA$_A$R PAMs bind to this site at concentrations similar to those necessary for GABA$_A$R enhancement, but we also identified potent steroid GABA$_A$R PAMs that do not bind to this site. High affinity binding depends on the presence of a free 3α-OH and is highly sensitive to the nature of the substitution at the C-17 position. 3-Deoxy-5α-P and steroids with an –OH in place of the carbonyl at C-20 of 3α5α-P enhance GABA responses with potencies similar to 3α5α-P (20, 30, 43), but their binding affinities for the β$^+$–α$^-$ steroid site are reduced by more than 1000-fold. These potent steroid PAMs that do not bind to the β$^+$–α$^-$ steroid site should serve as useful lead compounds for the development of novel reagents to identify additional GABA$_A$R steroid-binding sites.

Structural determinants for binding to the β$^+$–α$^-$ subunit interface steroid site

Because the β subunit amino acids photolabeled by [³H]21-*p*TFDBzoxy-AP were located within a common binding pocket at the β$^+$–α$^-$ subunit interface, characterization of the effects of nonradioactive steroids on GABA$_A$R photolabeling at the level of the β subunit could be used to determine the affinities (IC$_{50}$ values) of nonradioactive drugs for that site. We did not identify any nonsteroidal GABA$_A$R PAMs that inhibited photolabeling, including drugs varying in size from propofol to ivermectin that bind to the adjacent etomidate site at the β$^+$–α$^-$ subunit interface. Many steroid 3α-OH GABA$_A$R PAMs were potent inhibitors of [³H]21-pTFDBzoxy-AP photolabeling, reducing β subunit photolabeling maximally to the same extent as 30 μM 3α5α-P with a concentration dependence characterized by a Hill coefficient of 1. The simplest interpretation of this pattern of inhibition is that it results from competitive interactions at a common binding site. For α1β3 and α1β3γ2 GABA$_A$Rs, the IC$_{50}$ values for 5β-isomers differed by less than a factor of 2 from those for 3α5α-P, 3α5α-THDOC, and alphaxalone (Tables 1 and 4), and the IC$_{50}$ values for inhibition of photolabeling were within a factor of 2 of EC$_{50}$ values reported for enhancement of GABA responses (12, 23, 45). A similar good correlation between photolabeling inhibition IC$_{50}$ and GABA$_A$R enhancement EC$_{50}$ was seen for many substituted pregnanolones, including those acting *in vivo* as an anesthetic (Org20599), anti-convulsant (ganaxolone), or antidepressant (SAGE-217) (Tables 3 and 5).

Our results establish that high affinity binding to the GABA$_A$R β$^+$–α$^-$-binding site depends critically on the presence of a free 3α-OH, consistent with the inactivity of 3β-OH steroids, 3-oxo-5α-P, and 3α-acetyl-5α-P as GABA$_A$R PAMs (9–11, 28). We found that they bound at least 1000-fold more weakly than 3α5α-P. 3-Deoxy-5α-P also did not bind to this site, despite the fact that it acts as a GABA$_A$R PAM with a

Table 3
Inhibition of [³H]21-*p*TFDBzox-AP photolabeling by substituted 3α-OH pregnan steroid GABA$_A$R PAMs

	R_1	C-5	R_2	R_3	[³H]21-*p*TFDBzoxy-AP[a] IC$_{50}$ (n)	GABA enhancement[b] EC$_{50}$
					*μ*M	*μ*M
Org-20599 C-2:	-H	α	-CH$_3$	-COCH$_2$Cl	0.2 ± 0.02 (4)	1.2
Ganaxolone	-CH$_3$	α	-CH$_3$	-COCH$_3$	0.26 ± 0.04 B_{ns} = 29 ± 2% (8)	0.2
SAGE-217	-CH$_3$	β	-H		0.51 ± 0.07 (4)	0.4
3β-CH$_3$OCH$_2$-THDOC	-CH$_2$OCH$_3$	α	-CH$_3$	-COCH$_2$OH	2.1 ± 0.3 (6)	ND[c]
CCD-3693	-CF$_3$	β	-H	-COCH$_3$	0.95 ± 0.1 (4)	0.2[d]
UCI-50027	-CH$_3$	α	-CH$_3$		10.6 ± 1.5 (4)	1.2

[a] IC$_{50}$ (±S.E.) values, the total drug concentrations resulting in 50% inhibition of α1β3 GABA$_A$R photolabeling, were determined by fit of the data of Fig. 8*A* to Equation 2 under "Experimental procedures," with n_H = 1 and B_{ns} = 0, or for ganaxlone with variable B_{ns}. n, number of experiments.
[b] EC$_{50}$ values for steroid enhancement of GABA responses of α1βγ GABA$_A$Rs expressed in oocytes, from the literature: Org20599 (37); ganaxolone (38); SAGE-217 (39); UCI-50027 (41).
[c] ND, not determined.
[d] CD-3693 enhancement of [³H]flunitrazepam binding (40).

potency similar to 3α5α-P (20). Thus, 3-deoxy-5α-P enhances GABA responses without binding to this site.

We found substitutions at the steroid C-17 position that were unexpectedly important determinants of binding to the β$^+$–α$^-$ site. Early studies of 3α-OH steroids as GABA$_A$R PAMs established that the C-20 carbonyl of 3α5α-P was not essential, because androsterone (3α5αA-17-one) and pregnan-3α,20-diols were potent PAMs (11, 30, 43). The C-20 carbonyl is also not essential for binding to the β$^+$–α$^-$ site, because 3α5α-A and 3α5β-P-20-deoxy, PAMs with an –H or β-ethyl at C-17, bound with high affinity (Table 4). However, two potent PAMs, 5α-pregnan-3α,20α-diol and 5β-pregnan-3α,20β-diol, did not bind to the β$^+$–α$^-$ site at concentrations 100-fold higher than necessary for GABA$_A$R enhancement. 3α5α-A-17α-ol, with an α–OH at C-17, also did not bind to the β$^+$–α$^-$ site. However, this may not be simply a consequence of the -OH, because 3α5α-A-17β-ol is a PAM (50), as are other steroids with a C-17 side chain in a β-configuration (11, 51).
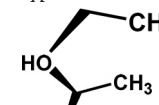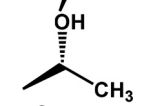
Although many 3α-OH steroid PAMs potently inhibited GABA$_A$R photolabeling to the same extent as 3α5α-P and with a concentration dependence characterized by a Hill coefficient of 1, ganaxalone and 3α5αA-17-one were exceptions. Ganaxolone was a potent inhibitor (IC$_{50}$ = 0.3 *μ*M), but at high concentrations, maximal inhibition (B_{ns} = 29 ± 2%) was less than that seen in the presence of 3α5α-P (B_{ns} = 0%), whereas other PAMs with 3β-substituents inhibited fully. For 3α5αA-17-one, which enhances α1β2γ GABA$_A$R responses with an EC$_{50}$ of ~3 *μ*M (52), inhibition was fit equally well either to n_H = 1 and variable B_{ns} (IC$_{50}$ = 5 ± 2 *μ*M, B_{ns} = 63 ± 3%) or with B_{ns} equal to 0 and a variable Hill coefficient (IC$_{50}$ = 700 ± 390 *μ*M, n_H =

0.32 ± 0.05). There was no evidence that the partial inhibition resulted from limited solubility of these two steroids in the detergent/lipid environment used for GABA$_A$R purification, and further studies are required to clarify the mechanism of inhibition.

Mode of steroid binding at the β$^+$–α$^-$ steroid site

Our photolabeling results establish that 21-*p*TFDBzoxy-AP binds in heteromeric GABA$_A$Rs at the β$^+$–α$^-$ subunit interface. Based upon computational docking, in its most energetically favorable binding mode, 21-*p*TFDBzoxy-AP's photoreactive diazirine is in proximity to the photolabeled amino acids at the cytoplasmic surface of the TMD and the 3α-OH is in proximity to α1Gln-242 and α1Trp-246. Thus, 21-*p*TFDBzoxy-AP binds at the β$^+$–α$^-$ subunit interface site in an orientation similar to that of 3α5α-THDOC, 3α5β-P, or alphaxalone at α$^+$–α$^-$ subunit interfaces in the crystal structures of homopentameric, chimeric receptors with GABA$_A$R α subunit TMDs (22–24). Consistent with this mode of binding, positive modulation of GABA responses by 21-*p*TFDBzoxy-AP is lost in the α1Q242W mutant receptor (27). Although direct interactions between the free 3α-OH and αGln-242 were predicted based upon the loss of 3α5α-P PAM activity seen for substitutions at αGln-242 (19), substitutions at αGln-242 also caused loss of PAM activity for 3-deoxy-5α-P (20), a PAM that did not inhibit [³H]21-*p*TFD-Bzoxy-AP photolabeling. This discrepancy indicates that substitutions at αGln-242 can interfere with PAM activity even for steroids that do not bind to the β$^+$–α$^-$ site, and the GABA$_A$R amino acids interacting directly with the 3α-OH remain to be determined.

Table 4
Inhibition of [³H]21-*p*TFDBzox-AP photolabeling by C-17 substituted 3α-OH steroid GABA_AR PAMs

Steroid[a]	C-5	R	[³H]21-pTFDBzoxy-AP[b] IC$_{50}$ (n)	GABA enhancement[c] EC$_{50}$
			μM	μM
21-*p*TFDBzox-AP	α	-COCH$_2$OCOBzTFD	0.21 ± 0.02	2.7
3α5β-A (A2150)	α	-H	8.7 ± 1.0 (6)	0.3
3α5β-P-20-deoxy (P7800)	β		4.2 ± 0.5 (4)	ND[d] (0.3)[e]
5α-Pregan3α,20α-diol (P1950)	α		>>300 (3)	0.2
5β-Pregnan3α,20β-diol (P6050)	β		>>300 (4)	2
3α5α-A-17-one (androsterone, A2420)	α	=O	~700 ± 400 (n_H = 0.35) (6)	~3
3α5α-A-17α-ol (A1150)	α	⸗OH	>300 (4)	ND
17-PA (5αA3α-ol,16-ene, 17-C$_6$H$_5$)	α	-C$_6$H$_5$	85 ± 13 (n_H = 0.3 ± 0.03) (4)	29 ± 5[f]

[a] Catalog numbers are indicated for steroids from Steraloids (A/P-xxxx).
[b] IC$_{50}$ (±S.E.) values, the total drug concentrations resulting in 50% inhibition of GABA_AR photolabeling, were determined as described under "Experimental Procedures" from data of Fig. 8B. *n*, number of experiments.
[c] EC$_{50}$ values for steroid enhancement of GABA responses of α1βγ GABA_ARs expressed in oocytes, from the literature: 21p-TFD-Bzoxy-AP (27); 3α5α-A (67); 5α-pregnan-3α,20α-diol and 5β-pregnan-3α,20β-diol (43); 3α5αA-17-one (52).
[d] ND, not determined.
[e] EC$_{50}$ for GABA_AR enhancement by 3α5α-P-20-deoxy (67).
[f] EC$_{50}$ for enhancement of [³H]muscimol binding (Fig. 2).

Based upon competition photolabeling, the presence of a free –OH at C-20 is as deleterious for binding to the β⁺−α⁻ site as is its absence at the C-3 position, even though a free hydroxyl group at C-21 (3α5α-THDOC) or certain bulky substitutions (21-*p*TFDBzoxy-AP, SAGE-217) are well-tolerated. Just as the high affinity binding associated with the 3α-OH must result from specific interactions with GABA_AR amino acids, the 1000-fold reduction of binding affinity (IC$_{50}$) for the pregnane diols compared with 3α5α/β-P is likely to result from energetically unfavorable interactions between a C-20 hydroxyl and GABA_AR amino acids in the β⁺−α⁻ interface steroid-binding site. If a pregnan-3α,20α/β-diol binds to the β⁺−α⁻ steroid site in the same orientation as alphaxalone or pregananolone in the crystal structures of chimeric receptors with α subunit TMDs (23, 24), the C-20 hydroxyl would be in proximity to β3Phe-301 in βM3, the position equivalent to α1Thr-206/α5Thr-309 that is in proximity to the C-20 carbonyl of alphaxalone and pregnanolone. Simple solubility considerations cannot account for the loss of binding, because incorporation of a hydroxyl residue instead of a carbonyl group increases the octanol-water partition coefficient calculated by the ALOGPS 2.1 program (RRID: SCR_018786) for any of the steroids tested by less than a factor of two, whereas 3α5β-P binds 7-fold more tightly and 5β-pregnan-3α,20β-diol binds >100-fold more weakly than 3α5β-P-20-deoxy (Table 4). Thus, the carbonyl at C-20 allows for favorable energetic interactions with GABA_AR amino acids not possible for a hydroxyl function.

In contrast to the differential effect on binding affinity seen for incorporation of a carbonyl or hydroxyl at C-20, direct incorporation of a carbonyl (androsterone) or a hydroxyl (3α5αA-17α-ol) on the steroid ring system at C-17 weakens binding by more than 50-fold compared with 3α5α-A. Likewise, the presence of a carbonyl (renanolone) or a hydroxyl (3α5β-P-11β-OH) at C-11 weakens binding by 20- and 300-fold compared with 3α5β-P. Because incorporation of a carbonyl or a hydroxyl will decrease the steroid partition coefficient by 10-30–fold, the decreased affinities (increased IC$_{50}$ values, measured as the total steroid concentration) for these steroids may result in large measure from their decreased hydrophobicity and lipid partitioning rather than from energetically unfavorable specific interactions of the carbonyl or hydroxyl with the GABA_AR.

Additional binding sites for steroid PAMs

Our sequencing results established that the β subunit amino acids photolabeled most efficiently by [³H]21-*p*TFDBzoxy-AP all contribute to the steroid-binding site at the β⁺−α⁻ subunit interface. Although we did not identify photolabeled amino acids that would contribute to other steroid-binding sites, our competition photolabeling results identified three potent PAMs (EC$_{50}$ <10 μM, 3-deoxy-5α-P, 5α-pregnan-3α,20α-diol, and 5β-pregnan-3α,20β-diol) that did not bind to this site. The absence of an α hydroxyl at C-3 at one end of the steroid ring system or the presence of a hydroxyl at C-20, 10 Å away at the other end of the ring system, prevents binding to the β⁺−α⁻ steroid site. The presence of the 3α-OH is insufficient to overcome unfavorable interactions at the other end of the molecule. It remains to be determined whether one or more of these

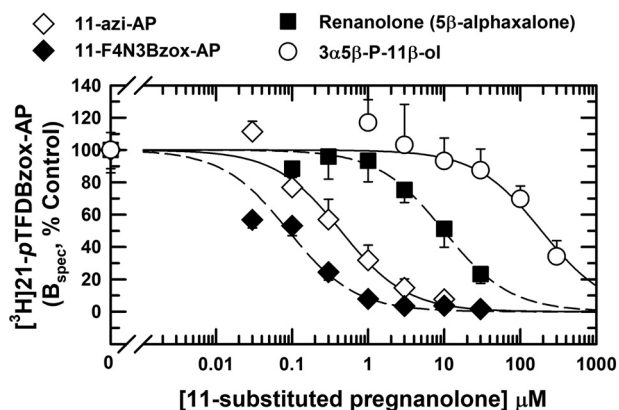**Figure 9. Effects of substituents at C-11 on steroid binding affinity for the [³H]21p-TFDBzox-AP site in α1β3 GABA_ARs.** GABA_ARs were photolabeled in the presence of GABA and the indicated concentrations of C_{11}-substituted derivatives of 3α5α-P (the photoreactive anesthetics 11-azi-AP and 11-F4N3Bzox-AP) or 3α5β-P (renanolone and 3α5β-P-11β-ol). The chemical structures, IC_{50} values determined from the concentration dependence of inhibition, and the number of independent experiments are presented in Table 5. Covalent incorporation of ³H was determined by liquid scintillation counting of β3 subunits isolated by SDS-PAGE, and data from independent experiments were normalized and combined as described under "Experimental procedures" and in Fig. 4. The plotted data are the mean ± S.D. from the independent experiments.

"orphan" PAMs bind to the intrasubunit sites near the extracellular end of the TMD recently identified by photolabeling in αM4 by steroids containing photoreactive groups at C-21 or C-6 and in βM3 by a steroid containing a C-3α photoreactive group (25).

Antagonist steroids

Although early studies suggested that 3β-OH steroids competitively antagonize steroid enhancement of GABA_AR function (53–55), subsequent studies indicate that they noncompetitively inhibit GABA responses in the absence of enhancing steroids, acting in a manner more similar to the sulfated 3β-OH neurosteroids PS and DHEAS (12, 56). Although steroid PAMs generally enhance [³H]muscimol or [³H]flunitrazepam equilibrium binding (51, 57, 58), our results indicate that inhibitory 3β-OH steroids can modulate [³H]muscimol binding in 3 different ways. (i) The enhancement of binding seen for betaxalone and 3β5β-P indicates that those steroids stabilize the GABA_AR in a desensitized state with high affinity for [³H]muscimol. 17-PA, a 3α-OH androstene that does not inhibit GABA responses in the absence of a steroid PAM (31, 59), also enhanced [³H]muscimol binding. (ii) The lack of modulation seen for 3β5α-P and PS at concentrations as high as 100 μM suggests that they do not perturb the receptor conformational state. (iii) That DHEAS partially inhibits binding indicates that it stabilizes the receptor in a state with low affinity for [³H]muscimol, potentially a resting, closed channel state. The effects we observed for 3β5α-P, PS, and DHEAS are consistent with previous studies of [³H]muscimol binding to rat brain membranes (29, 60).

Our competition photolabeling results are consistent with functional studies indicating that free and sulfated 3β-OH steroids inhibit GABA responses without binding to the same site as steroid PAMs. Thus, PS, 3β5α-P, and 3β5β-P inhibit GABA

responses with IC_{50} values of less than 5 μM (12, 61), but any inhibition of [³H]21-pTFDBzoxy-AP, photolabeling, if it occurred, would be characterized by IC_{50} values greater than 300 μM. Betaxalone was a possible exception, because inhibition (IC_{50} = 175 μM) occurred at similar concentrations as enhancement of [³H]muscimol binding (EC_{50} = 50 μM). However, the concentration dependence of inhibition of photolabeling (n_H = 0.5) was inconsistent with a simple model of direct completion for the [³H]21-pTFDBzoxy-AP–binding site.

Conclusions

We have shown that [³H]21-pTFDBzoxy-AP, a photoreactive steroid and GABA_AR PAM, binds with high affinity in the β^+−α^- subunit interface of heteromeric, human, full-length α1β3 and α1β3γ2L GABA_ARs in a site homologous to that revealed in crystal structures of chimeric homomeric pentameric ligand-gated ion channels of the same superfamily. We used competition photolabeling to establish that the steroid structure–activity relationships of this site parallel that observed in many functional pharmacological studies. These studies also reveal that some potent PAMs, such as 3α-deoxy-5α-P and pregnan-3α,20-diols, bind to a different site or sites, Thus, [³H]21-pTFD-Bzoxy-AP is a useful tool for the development of steroids that selectively target specific sites on GABA_ARs including those with other subunit compositions.
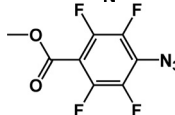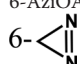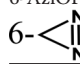
Experimental procedures

Materials

Nonradioactive 21-pTFDBzox-AP and [³H]21-pTFDBzox-AP (21.8 Ci/mmol, stored at −20 °C in ethanol at 1 mCi/ml) were prepared as described previously (27). The 21-pTFDBzox-AP UV spectrum was characterized by a major absorption peak at 241 nm (ε = 16,160 M^{-1} cm^{-1}) with a secondary, diazirine band with absorption maximum at 347 nm (ε = 360 M^{-1} cm^{-1}). [³H]Azietomidate (19 Ci/mmol, 53 μM in ethanol) and nonradioactive and [³H]R-mTFD-MPAB (38 Ci/mmol, 26 μM) were also synthesized and tritiated previously (33, 62). 11-Azi-AP and 11-F₄N₃Bzox-AP were prepared as described previously (45). UCI-50027 (41) and CCD-3693 (40) were gifts from Drs. Derk Hogenkamp and Kelvin Gee (Department of Pharmacology, College of Medicine, University of California, Irvine). 3β-CH₃OCH₂-THDOC (42) was a gift from Drs. Shuo enTsai and Fung Fuh Wong (School of Pharmacy, China Medical University, Taichung, Taiwan). Other nonradioactive steroids were from commercial sources, most from Research Plus or Steraloids, but also from Tocris (3α5α-P, Org20599, and 17-PA), Santa Cruz Biotechnology (PS), Sigma-Aldrich (ganaxolone, DHEAS, 3α5β-P, and alphaxalone), and Med-ChemExpress (Sage-217). Chemical structures of steroids tested are presented in Fig. S1. Ivermectin was from Tocris. o-Phthalaldehyde and cyanogen bromide were from TCI Chemicals and Alfa Aesar, respectively. Endoproteinase Lys-C was from New England Biolabs.

Human α1β3 and α1β3γ2 GABA_ARs with the α1 subunits containing a FLAG epitope at the N terminus of the mature subunit were expressed in tetracycline-inducible, stably transfected HEK293-TetR cell lines, and purified from detergent

Table 5

Inhibition of [³H]21-*p*TFDBzox-AP photolabeling by C-11 substituted pregnanolone GABA$_A$R PAMs

	R	C-5	[³H]21-*p*TFDBzoxy-AP[a] IC$_{50}$ (n)	GABA enhancement[b] EC$_{50}$
			μM	*μM*
Alphaxalone	=O	α	4.6 ± 0.7 (4)	2.2
11-Azi-AP		α	0.44 ± 0.06 (4)	0.2 ± 0.1
11-F$_4$N$_3$Bzox-AP		α	0.09 ± 0.01 (4)	0.5 ± 0.2
6-AziOAP	=O	α	44[c]	25[c]
Renanolone (Res Plus 3183-16)	=O	β	10 ± 1.5 (4)	3.6
3α5β-P-11β-ol (Res Plus 3159-16)	-OH	β	190 ± 32 (6)	>300
6-AziOP	=O	β	>100[c]	37[c]

[a] IC$_{50}$ (±S.E.) values, the total drug concentrations resulting in 50% inhibition of α1β3 GABA$_A$R photolabeling, were determined as described under "Experimental Procedures" from data of Fig. 9 or Ref. 27. *n*, number of experiments.
[b] Literature EC$_{50}$ values for steroid enhancement of GABA responses of α1β3γ2 GABA$_A$Rs expressed in oocytes (alphaxalone, 11-Azi-AP, and 11-F$_4$N$_3$Bzox-AP (45)) or for enhancement of [³H]flunitrazepam binding to rat brain membranes (renanolone (58); 3α5β-pregnan-11β-ol (68)).
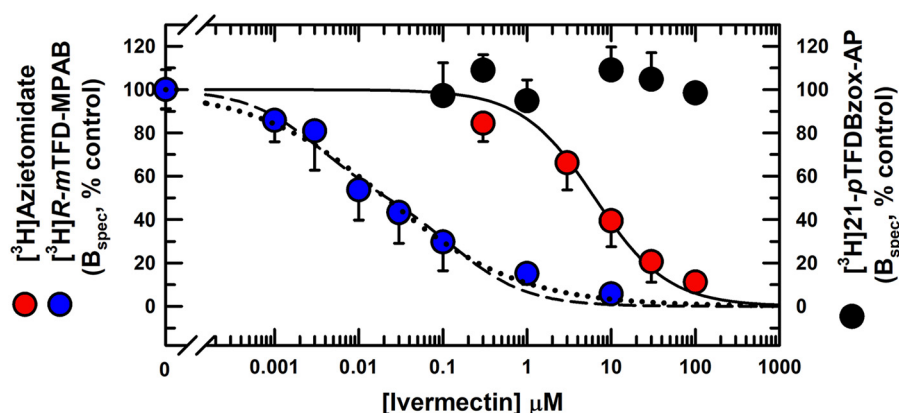[c] From Ref. 27, EC$_{50}$ for enhancement of [³H]muscimol binding.

Figure 10. Ivermectin binds to the $\alpha^+/\gamma^+-\beta^-$ ([³H]R-mTFD-MPAB) and $\beta^+-\alpha^-$ ([³H]azietomidate) intersubunit anesthetic sites without altering binding of [³H]21p-TFDBzox-AP to its $\beta^+-\alpha^-$ intersubunit site. α1β3γ2 GABA$_A$Rs were photolabeled in the presence of GABA with varying concentrations of ivermectin. After SDS-PAGE, ³H incorporation into GABA$_A$R subunits was determined by liquid scintillation counting. For each independent experiment, non-specific photolabeling was determined in the presence of 30 μM 3α5β-P ([³H]21p-TFDBzox-AP (n = 4)), 60 μM nonradioactive R-mTFD-MPAB ([³H]R-mTFD-MPAB (n = 3)), or 300 μM etomidate ([³H]azietomidate (n = 3)). For each photoprobe, specific binding in ³H cpm was determined for each independent experiment and normalized to the specific binding in the control condition, and data from the independent experiments were pooled. The plotted data are the mean ± S.D. from the independent experiments. When fit to Equation 2, for [³H]azietomidate, IC$_{50}$ = 6.4 ± 1.0 μM, n_H =1 (R² = 0.93). For [³H]R-mTFD-MPAB, IC$_{50}$ = 21 ± 5 nM and n_H = 0.55 ± 0.08 (*dots*, R² = 0.92) or when fit to a two site model ($B(x) = \frac{0.5(B_o - B_{ns})}{1 + \left(\frac{x}{IC_{50H}}\right)} + \frac{0.5(B_o - B_{ns})}{1 + \left(\frac{x}{IC_{50L}}\right)} + B_{ns}$; *dashed line*), IC$_{50H}$ = 3 ± 1 nM, IC$_{50L}$ = 140 ± 64 nM (R² = 0.91).

extracts as described previously (13, 62–64) by use of an anti-FLAG antibody column. In brief, cells were grown for 72 h on 15-cm plates at 37 °C, induced with tetracycline and 5 mM sodium butyrate for 24 h, then harvested and lysed as described (63), with membrane pellet suspensions flash frozen in liquid nitrogen and stored at −80 °C. α1β3 and α1β3γ2 GABA$_A$Rs were expressed at ~30 and 5-10 pmol of [³H]muscimol-binding sites per mg of membrane protein, respectively. For GABA$_A$R purifications, membranes (1 mg of protein/ml) were solubilized for 2.5 h in purification buffer (13) supplemented

with 30 mM *n*-dodecyl β-D-maltopyranoside. Column wash and elution buffers contained 0.2 mM asolectin and 5 mM CHAPS. After elution from columns in the presence of 5 mM FLAG peptide (elutions 1 and 2, 13 ml each), aliquots were characterized for [³H]muscimol binding. Membranes from 30 plates of α1β3 GABA$_A$Rs (10-15 nmol of binding sites) yielded 2-3 nmol of purified receptor (60-110 and 30-40 nM binding sites in elutions 1 and 2). Membranes from 60 to 70 plates of α1β3γ2 GABA$_A$Rs contained 4-5 nmol of binding sites and yielded ~1 nmol of purified receptor (50-60 nM and 20-30 nM binding sites in

elutions 1 and 2). Aliquots of purified GABA_ARs were stored at −80 °C until use.

[³H]Muscimol binding

Membrane homogenates were prepared as described (63) from HEK 293 TetR cells expressing α1β3 GABA_ARs. Membrane suspensions (50 µg of protein/ml in 2 ml of assay buffer (200 mM KCl, 1 mM EDTA, 10 mM phosphate buffer, pH 7.4)) were equilibrated with 2 nM [³H]muscimol (PerkinElmer Life Sciences) and various concentrations of steroid for 1 h at 4 °C and then filtered in quadruplicate on Whatman GF/B glass fiber filters that had been pretreated with 0.5% polyethyleneimine for 1 h. After being washed twice with 5 ml of cold assay buffer, filters were dried and ³H retention was determined by liquid scintillation counting. Nonspecific binding was determined in the presence of 1 mM GABA. The modulation results are presented as the percentage of the specifically bound [³H]muscimol over that without steroid. The plotted data are the mean ± S.D. of pooled data from 2 to 4 independent experiments, and the full data sets were fit to Equation 1 to determine values of EC_50, n_H, and maximal enhancement.

$$B\%(x) = \frac{Bmax - 100}{1 + \left(\frac{EC_{50}}{x}\right)^{nH}} + 100 \qquad \text{(Eq. 1)}$$

GABA_AR photolabeling

Purified α1β3 or α1β3γ2 GABA_ARs were photolabeled with [³H]21-pTFDBzox-AP in the presence of 300 µM GABA on an analytical scale (50 µl/gel lane, ~2 pmol of [³H]muscimol-binding sites) or for α1β3 GABA_ARs on a preparative scale (1.5-2 ml, 60-170 pmol of [³H]muscimol sites per condition). Appropriate volumes of [³H]21-pTFDBzox-AP were dried down under an argon stream and resuspended with gentle vortexing for 30 min at 4 °C in freshly thawed GABA_AR aliquots. Final concentrations of [³H]21-pTFDBzox-AP varied between 0.5 and 1 µM for α1β3 GABA_AR photolabelings and 0.5 and 1.5 µM for α1β3γ2 GABA_ARs. For preparative scale labeling, the resuspended sample was divided into two equal aliquots for determination of photolabeled amino acids in the absence or presence of 30 µM 3α5α-P. Both samples contained 0.5% (v/v) methanol. Samples were incubated at 4 °C for 30 min, placed into 3.5 cm diameter plastic Petri dishes, and irradiated using a Spectroline model EN-280L 365-nm lamp for 30 min on ice from a distance of 1 cm. For analytical photolabeling assays, a 1-µl glass syringe (Hamilton 86200) was used to add 0.25 µl (0.5%) of the steroid/drug to be tested to a 10-µl aliquot of GABA_AR in glass vials (CERT5000-69LV, ThermoFisher Scientific) followed by addition of 40-µl aliquots of GABA_AR equilibrated with [³H]21-pTFDBzox-AP. Samples were vortexed, incubated on ice for 45 min, transferred to 96-well plates, and then irradiated for 30 min at 365 nm. Most stock solutions of nonradioactive steroids were prepared in ethanol at 60 mM, or at 150 (DHEAS and PS), 20 (3α5β-THDOC), or 6 mM (Org20599). Stock solutions of 11-aziAP (11 mM) and 11-F₄N₃Bzox-AP (7.6 mM) were prepared in methanol. Stock solutions in DMSO were prepared at 150 (3β5β-P, 5β-pregnan-3α,20β-diol, 3α5α-A, 3α5αA-17α-

ol, and 3α5α-A-17-one), 60 (3-acetyl-5α-P, 3-deoxy-5α-P, 5α-pregnan-3α,20α-diol, 5β-pregnan-3α,11β-diol-20-one, and SAGE-217), or 22 mM (21-pTFDBzox-AP). The final concentrations of ethanol, methanol, or DMSO during labeling were 0.5, 0.5, or 0.2% (v/v), respectively.

After photolabeling, GABA_AR subunits were separated by SDS-PAGE as described (13), and gel bands containing α/γ (56 kDa) and β (59/61 kDa) subunits were identified by Gel Code Blue Safe Protein Stain (ThermoFisher Scientific) for analytical labelings (26). For analytical scale experiments, [³H]21-pTFDBzox-AP incorporation was measured by scintillation counting of excised gel bands (in ³H cpm) or by fluorography (13). For preparative scale experiments, gel bands of interest were excised and eluted passively in elution buffer (100 mM NH₄HCO₃, 2.5 mM DTT, 0.1% SDS, pH 8.4) for 3 days at room temperature. The eluates were filtered and concentrated, and the proteins in the eluate were precipitated (75% acetone, overnight at −20 °C) and then resuspended in digestion buffer (15 mM Tris, 0.5 mM EDTA, 0.1% SDS, pH 8.4).

Quantitation of concentration dependence of inhibition of photolabeling

The concentration dependence of inhibition of ³H incorporation into GABA_AR subunits was fit by nonlinear least squares to Equation 2,

$$B(x) = \frac{B_0 - B_{ns}}{1 + \left(\frac{x}{IC_{50}}\right)^{nH}} + B_{ns} \qquad \text{(Eq. 2)}$$

where, $B(x)$ is the ³H cpm incorporated into a subunit gel band at a total inhibitor concentration of x. B_0 is incorporation in the absence of inhibitor, B_{ns} is the nonspecific incorporation, IC_50 is total inhibitor concentration that reduces the specific incorporation by 50%, and n_H is the Hill coefficient. For [³H]21-pTFDBzox-AP, nonspecific photolabeling was determined in the presence of 30 µM 3α5α-P. IC_50 values were determined for inhibition of [³H]21-pTFDBzox-AP incorporation in the β subunit gel bands (59/61 kDa) that reflects photolabeling of residues at the β⁺−α⁻ subunit interface at the cytoplasmic end of the TMD (see "Results"). For [³H]azietomidate and [³H]R-mTFD-MPAB, IC_50 values were determined for inhibition of photolabeling in the α (56 kDa) and β (59/61 kDa) subunit gel bands, respectively, which reflect labeling of α1Met-236 and β3Met-227 (13, 62). For each drug tested, data from 4 to 6 experiments, using at least 2 different GABA_AR purifications, were combined by normalizing (as %) the specific incorporation ($B_x − B_{ns}$) at each concentration to the specific incorporation in the absence of drug ($B_0 − B_{ns}$) for each experiment individually. The data plotted in the figures are the mean ± S.D. values of the normalized specific data from n experiments. The full normalized data sets were fit (GraphPad Prism 7.0 or SigmaPlot 11.0) using Equation 2. For all fits, the best fit values (± S.E.) of the variable parameters and the number of experiments are reported in the tables, with the plotted curves calculated from those parameters. Unless noted otherwise, the reported IC_50 values and calculated curves are for fits with $B_{ns} = 0$ and $n_H = 1$. Parameters

from fits with variable n_H or variable B_{ns} are not reported unless n_H was less than 0.8 or B_{ns} was greater than 15%. The extra sum of the squares principle (*F* test, $\alpha = 0.05$) was used to determine whether a variable n_H provided a statistically favored fit compared with $n_H = 1$ (null hypothesis), or whether IC$_{50}$ values for a drug were the same (null hypothesis) or different for $\alpha1\beta3$ and $\alpha1\beta3\gamma2$ GABA$_A$Rs.

Enzymatic and chemical fragmentation

$\alpha1$ and $\beta3$ subunits isolated by SDS-PAGE from $\alpha1\beta3$ GABA$_A$Rs photolabeled on a preparative scale were digested with Endo Lys-C (3-5 µg, 3 days, 20 °C), which produces fragments beginning at the N termini of each subunit's M1, M3 and M4 helices that can be separated and purified by rpHPLC (13). To cleave at the C-terminal side of methionines, samples already loaded onto sequencing supports were treated with cyanogen bromide as described (65, 66).

HPLC purification and protein microsequencing

Subunit digests were fractionated by rpHPLC on an Agilent 1100 binary pump system using a Brownlee C4 Aquapore column (100 × 2.1 mm, 7-µm particle size) at 40 °C with an upstream guard column (Newguard RP-2). The aqueous solvent contained 0.08% TFA and the organic solvent contained 60% acetonitrile, 40% isopropyl alcohol, 0.05% TFA. Elution was achieved using a nonlinear gradient increasing from 5 to 100% organic solvent over 80 min at a flow rate of 0.2 ml/min. Fractions of 0.5 ml were collected, and 10% aliquots were assayed for determination of ^{3}H. Fractions of interest were pooled for sequencing and drop-loaded at 45 °C onto Micro TFA glass fiber sequencing filters (Applied Biosytems) that were treated after loading with Bio-brene Plus (Applied Biosystems).

Samples were sequenced on an Applied Biosystems Procise 492 Protein sequencer programed to use 2/3 (~80 of 120 µl) of the material from each cycle of Edman degradation for PTH-derivative identification and quantitation and to collect 1/3 for ^{3}H determination by liquid scintillation counting. For some samples, sequencing was interrupted at a designated cycle for treatment of the sequencing filter with *o*-phthalaldehyde (35, 36) to prevent further sequencing of any peptide not containing a proline at that cycle. The amount of PTH-derivative released (in picomoles) for a given residue was quantified using their peak height in the chromatogram, background-subtracted, compared with a standard peak, and the PTH-derivatives released for the detected peptide were fit to the equation,

$$F(x) \quad = \quad I_0 \times R^x \qquad \text{(Eq. 3)}$$

where $F(x)$ is the pmol of the amino acid in cycle x, I_0 is the calculated initial amount of the peptide, and R is the repetitive yield. The 1st residue in the peptide as well as Cys, Trp, His, and Ser were not used in the calculation due to known problems with their quantitation. The efficiency of photolabeling (*E* in cpm/pmol) at a labeled amino acid in cycle x was calculated by the equation,

$$E(x) = \frac{2 \times (cpm_{(x)} - cpm_{(x-1)})}{I_0 \times R^x} \qquad \text{(Eq. 4)}$$

where cpm_x is the ^{3}H released in cycle x.

Molecular modeling and computational docking

For computational docking studies, we used the recently solved cryo-EM structure of a desensitized state of $\alpha1\beta3\gamma2$L GABA$_A$R (PDB 6I53) (18) in a lipid-nanodisc with a bound positive allosteric modulator megabody in the extracellular domain. This structure was determined from GABA$_A$Rs purified from the same cell line as that used in our photolabeling studies, a cell line expressing full-length receptor subunits with intact cytoplasmic domains. Although most of the ~120 amino acids comprising each subunit cytoplasmic domain were not resolved in this structure, the locations of 4 of the 5 amino acids specifically photolabeled by [^{3}H]21-pTFDBzox-AP were resolved. In contrast, only the photolabeled $\beta3$Arg-309 was resolved in 5 other structures using the same source of GABA$_A$Rs that were determined in the presence of GABA, picrotoxinin, or bicuculline (17).

Docking of 21-pTFDBzox-AP and other steroids to the PDB 6I53 model was performed using the Discovery Studio CDOCKER module. Potential binding sites at each subunit interface of the PDB 6I53 structure were defined by 14-Å radius binding site spheres centered by the position of $3\alpha5\alpha$-THDOC molecules overlaid (Discovery Studio: Tools: Superimpose Proteins: Sequence Alignment) from the PDB 5OSB structure (after removal of the extracellular domain and cytoplasmic linker). For docking, a structure of 21-pTFDBzox-AP was created by appropriate additions at the 21 position of $3\alpha5\alpha$-THDOC (PubChem structure CID No. 101,771). Four copies of 21-pTFDBzox-AP, differing by rotations of ~180°, were seeded into the binding site spheres. The 50 lowest energy solutions (simulated annealing with full potential minimization) were collected for each molecule from 50 random conformations (high temperature molecular dynamics) and 50 randomized orientations within the sphere (*i.e.* 2,500 attempted dockings per molecule). In two independent docking runs, we found that 21-pTFDBzox-AP was predicted to bind most favorably at the $\gamma\beta^+-\alpha^-$ subunit interface with the lowest CDocker interaction energy (−49.17 kcal/mol) at that site 4.5 kcal/mol more favorable than at the $\beta^+-\alpha^-\gamma$–binding site and more than 10 kcal/mol more favorable than at the homologous $\alpha^+-\gamma^-$, $\alpha^+-\beta^-$, or $\gamma^+-\beta^-$ intersubunit sites. At the $\gamma\beta^+-\alpha^-$ site, for the energetically most favored solution and 56% of all collected solutions, 21-pTFDBzox-AP adopted a common orientation with the 3α-OH directed toward $\alpha1$Gln-242 and the aromatic diazirine extending linearly from the steroid backbone into a groove between $\beta3$Arg-309 and $\beta3$Leu-417, residues photolabeled by [^{3}H]21-pTFDBzox-AP (see "Results"). $3\alpha5\alpha$-THDOC and $3\alpha5\alpha$-P were also predicted to bind in a similar orientation at the $\gamma\beta^+-\alpha^-$ site, with most favorable CDOCKER interaction energies of −40.6 and −35.0 kcal/mol. Although both molecules were predicted to bind in an orientation with the 3α-OH in proximity to $\alpha1$Gln-242, no consistent prediction was made concerning the energetic importance of a 3α-OH. For THDOC,

ॐASBMB

J. Biol. Chem. (2020) 295(33) 11495–11512 **11509**

the CDOCKER interaction energy for the 3α-OH isomer was 1.8 kcal/mol more favorable than for the 3β-epimer, whereas the interaction energy was 1.4 kcal/mol more favorable for 3β5α-P than for 3α5α-P.

Data availability

All data are contained within the article.

Author contributions—S. S. J., D. C. C., and J. B. C. conceptualization; S. S. J., D. C. C., X. Z., and K. W. M. investigation; S. S. J. and D. C. C. methodology; S. S. J., K. S. B., K. W. M., and J. B. C. writing-review and editing; X. Z., B. W., K. S. B., and K. W. M. resources; K. S. B., K. W. M., and J. B. C. funding acquisition; J. B. C. supervision; J. B. C. writing-original draft.

Conflict of interest—The authors declare that they have no conflicts of interest with the contents of this article.

Abbreviations—The abbreviations used are: 3α5α-P, allopregnanolone; 3α5β-P, pregnanolone; PAM, positive allosteric modulator; GABA$_A$R, γ-aminobutyric acid type A receptor; THDOC, tetrahydrocorticosterone; 21-*p*TFDBzox-AP, 21-[4-(3-(trifluoromethyl)-3H-diazirine-3-yl)benzoxy] allopregnanolone; *R-m*TFD-MPAB, (*R*)-5-allyl-1-methyl-5-(*m*-trifluoromethyl-diazirynylphenyl)barbituric acid; azietomidate, 2-(3-methyl-3*H*-diazirine-3-yl)ethyl (*R*)-1-(phenylethyl)-1H-imidazole-5-carboxylate; TMD, transmembrane domain; PS, pregnenolone sulfate; DHEAS, dehydroepiandrosterone sulfate; 17-PA, (3α5α)-17-phenylandrost-16-en-3-ol; Endo Lys-C, endoproteinase Lys-C; rpHPLC, reversed phase high performance liquid chromatography; PTH, phenylthiohydantoin; OPA, *o*-phthaldehyde; PDB, Protein Data Bank.

References

1. Belelli, D., and Lambert, J. J. (2005) Neurosteroids: Endogenous regulators of the GABA(A) receptor. *Nat. Rev. Neurosci.* **6,** 565–575 CrossRef Medline
2. Belelli, D., Hogenkamp, D., Gee, K. W., and Lambert, J. J. (2020) Realising the therapeutic potential of neuroactive steroid modulators of the GABA$_A$ receptor. *Neurobiol. Stress* **12,** 100207 CrossRef Medline
3. Reddy, D. S., and Estes, W. A. (2016) Clinical potential of neurosteroids for CNS disorders. *Trends Pharmacol. Sci.* **37,** 543–561 CrossRef Medline
4. Blanco, M.-J., La, D., Coughlin, Q., Newman, C. A., Griffin, A. M., Harrison, B. L., and Salituro, F. G. (2018) Breakthroughs in neuroactive steroid drug discovery. *Bioorg. Med. Chem. Lett.* **28,** 61–70 CrossRef Medline
5. Majewska, M. D., Harrison, N. L., Schwartz, R. D., Barker, J. L., and Paul, S. M. (1986) Steroid hormone metabolites are barbiturate-like modulators of the GABA receptor. *Science* **232,** 1004– 1007 CrossRef Medline
6. Puia, G., Santi, M. R., Vicini, S., Pritchett, D. B., Purdy, R. H., Paul, S. M., Seeburg, P. H., and Costa, E. (1990) Neurosteroids act on recombinant human GABA$_A$ receptors. *Neuron* **4,** 759–765 CrossRef Medline
7. Akk, G., Covey, D. F., Evers, A. S., Steinbach, J. H., Zorumski, C. F., and Mennerick, S. (2007) Mechanisms of neurosteroid interactions with GABA(A) receptors. *Pharmacol. Ther.* **116,** 35–57 CrossRef Medline
8. Hosie, A. M., Wilkins, M. E., and Smart, T. G. (2007) Neurosteroid binding sites on GABA(A) receptors. *Pharmacol. Ther.* **116,** 7–19 CrossRef Medline
9. Harrison, N. L., Majewska, M. D., Harrington, J. W., and Barker, J. L. (1987) Structure-activity relationships for steroid interaction with the γ-aminobutyric acid$_A$ receptor complex. *J. Pharmacol. Exp. Ther.* **241,** 346–353 Medline
10. Cottrell, G. A., Lambert, J. J., and Peters, J. A. (1987) Modulation of GABA$_A$ receptor activity by alphaxalone. *Br. J. Pharmacol.* **90,** 491–500 CrossRef Medline
11. Purdy, R. H., Morrow, A. L., Blinn, J. R., and Paul, S. M. (1990) Synthesis, metabolism, and pharmacological activity of 3α-hydroxy steroids which potentiate GABA-receptor-mediated chloride ion uptake in rat cerebral cortical synaptoneurosomes. *J.Med. Chem.* **33,** 1572–1581 CrossRef Medline
12. Wang, M. D., He, Y. J., Eisenman, L. N., Fields, C., Zeng, C. M., Mathews, J., Benz, A., Fu, T., Zorumski, E., Steinbach, J. H., Covey, D. F., Zorumski, C. F., and Mennerick, S. (2002) 3β-Hydroxypregnane steroids are pregnenolone sulfate-like GABA(A) receptor antagonists. *J. Neurosci.* **22,** 3366–3375 CrossRef Medline
13. Chiara, D. C., Jayakar, S. S., Zhou, X., Zhang, X., Savechenkov, P. Y., Bruzik, K. S., Miller, K. W., and Cohen, J. B. (2013) Specificity of intersubunit general anesthetic-binding sites in the transmembrane domain of the human α1β3γ2 γ-aminobutyric acid Type A (GABA$_A$) receptor. *J. Biol. Chem.* **288,** 19343–19357 CrossRef Medline
14. Forman, S. A., and Miller, K. W. (2016) Mapping general anesthetic sites in heteromeric γ-aminobutyric acid type a receptors reveals a potential for targeting receptor subtypes. *Anesth. Analg.* **123,** 1263–1273 CrossRef Medline
15. Akk, G., Bracamontes, J., Covey, D. F., Evers, A. R., Dao, T., and Steinbach, J. H. (2004) Neuroactive steroids have multiple actions to potentiate GABA$_A$ receptors. *J. Physiol.* **558,** 59–74 CrossRef Medline
16. Evers, A. S., Chen, Z.-W., Manion, B. D., Han, M., Jiang, X., Darbandi-Tonkabon, R., Kable, T., Bracamontes, J., Zorumski, C. F., Mennerick, S., Steinbach, J. H., and Covey, D. F. (2010) A synthetic 18-norsteroid distinguishes between two neuroactive steroid binding sites on GABA$_A$ receptors. *J. Pharmacol. Exp. Ther.* **333,** 404–413 CrossRef Medline
17. Masiulis, S., Desai, R., Uchański, T., Serna Martin, I., Laverty, D., Karia, D., Malinauskas, T., Zivanov, J., Pardon, E., Kotecha, A., Steyaert, J., Miller, K. W., and Aricescu, A. R. (2019) GABA$_A$ receptor signalling mechanisms revealed by structural pharmacology. *Nature* **565,** 454–459 CrossRef Medline
18. Laverty, D., Desai, R., Uchański, T., Masiulis, S., Stec, W. J., Malinauskas, T., Zivanov, J., Pardon, E., Steyaert, J., Miller, K. W., and Aricescu, A. R. (2019) Cryo-EM structure of the human α1β3γ2 GABA$_A$ receptor in a lipid bilayer. *Nature* **565,** 516–520 CrossRef Medline
19. Hosie, A. M., Wilkins, M. E., Da Silva, H. M. A., and Smart, T. G. (2006) Endogenous neurosteroids regulate GABA$_A$ receptors through two discrete transmembrane sites. *Nature* **444,** 486–489 CrossRef Medline
20. Akk, G., Li, P., Bracamontes, J., Reichert, D. E., Covey, D. F., and Steinbach, J. H. (2008) Mutations of the GABA-A receptor α1 subunit M1 domain reveal unexpected complexity for modulation by neuroactive steroids. *Mol. Pharmacol.* **74,** 614–627 CrossRef Medline
21. Ziemba, A. M., Szabo, A., Pierce, D. W., Haburcak, M., Stern, A. T., Nourmahnad, A., Halpin, E. S., and Forman, S. A. (2018) Alphaxalone binds in inner transmembrane β⁺-α⁻ interfaces of α1β3γ2 γ-aminobutyric acid type A receptors. *Anesthesiology* **128,** 338–351 CrossRef Medline
22. Laverty, D., Thomas, P., Field, M., Andersen, O. J., Gold, M. G., Biggin, P. C., Gielen, M., and Smart, T. G. (2017) Crystal structures of a GABA$_A$-

receptor chimera reveal new endogenous neurosteroid-binding sites. *Nat. Struct. Mol. Biol.* **24,** 977–985 CrossRef Medline

23. Miller, P. S., Scott, S., Masiulis, S., De Colibus, L., Pardon, E., Steyaert, J., and Aricescu, A. R. (2017) Structural basis for GABA_A receptor potentiation by neurosteroids. *Nat. Struct. Mol. Biol.* **24,** 986–992 CrossRef Medline

24. Chen, Q., Wells, M. M., Arjunan, P., Tillman, T. S., Cohen, A. E., Xu, Y., and Tang, P. (2018) Structural basis of neurosteroid anesthetic action on GABA(A) receptors. *Nat. Commun.* **9,** 3972 CrossRef Medline

25. Chen, Z. W., Bracamontes, J. R., Budelier, M. M., Germann, A. L., Shin, D. J., Kathiresan, K., Qian, M. X., Manion, B., Cheng, W. W. L., Reichert, D. E., Akk, G., Covey, D. F., and Evers, A. S. (2019) Multiple functional neurosteroid binding sites on GABA_A receptors. *PLoS Biol.* **17,** e3000157 CrossRef

26. Jayakar, S. S., Zhou, X. J., Chiara, D. C., Jarava-Barrera, C., Savechenkov, P. Y., Bruzik, K. S., Tortosa, M., Miller, K. W., and Cohen, J. B. (2019) Identifying drugs that bind selectively to intersubunit general anesthetic sites in the $\alpha1\beta3\gamma2$ GABA_AR transmembrane domain. *Mol. Pharmacol.* **95,** 615–628 CrossRef Medline

27. Wu, B., Jayakar, S. S., Zhou, X., Titterton, K., Chiara, D. C., Szabo, A. L., Savechenkov, P. Y., Kent, D. E., Cohen, J. B., Forman, S. A., Miller, K. W., and Bruzik, K. S. (2019) Inhibitable photolabeling by neurosteroid diazirine analog in the $\beta3$-subunit of human hetereopentameric type A GABA receptors. *Eur. J. Med. Chem.* **162,** 810–824 CrossRef

28. Peters, J. A., Kirkness, E. F., Callachan, H., Lambert, J. J., and Turner, A. J. (1988) Modulation of the GABA_A receptor by depressant barbiturates and pregnane steroids. *Br. J. Pharmacol.* **94,** 1257–1269 CrossRef Medline

29. Demirgören, S., Majewska, M. D., Spivak, C. E., and London, E. D. (1991) Receptor binding and electrophysiological effects of dehydroepiandrosterone sulfate, an antagonist of the GABA_A receptor. *Neuroscience* **45,** 127–135 CrossRef

30. Park-Chung, M., Malayev, A., Purdy, R. H., Gibbs, T. T., and Farb, D. H. (1999) Sulfated and unsulfated steroids modulate γ-aminobutyric acid_A receptor function through distinct sites. *Brain Res.* **830,** 72–87 CrossRef Medline

31. Mennerick, S., He, Y. J., Jiang, X., Manion, B. D., Wang, M. D., Shute, A., Benz, A., Evers, A. S., Covey, D. F., and Zorumski, C. F. (2004) Selective antagonism of 5α-reduced neurosteroid effects at GABA_A receptors. *Mol. Pharmacol.* **65,** 1191–1197 CrossRef Medline

32. Chiara, D. C., Dostalova, Z., Jayakar, S. S., Zhou, X., Miller, K. W., and Cohen, J. B. (2012) Mapping general anesthetic binding site(s) in human $\alpha1\beta3$ γ-aminobutyric acid type A receptors with [³H]TDBzl-Etomidate, a photoreactive etomidate analogue. *Biochemistry* **51,** 836–847 CrossRef Medline

33. Savechenkov, P. Y., Zhang, X., Chiara, D. C., Stewart, D. S., Ge, R., Zhou, X., Raines, D. E., Cohen, J. B., Forman, S. A., Miller, K. W., and Bruzik, K. S. (2012) Allyl *m*-trifluoromethyldiazirine mephobarbital: an unusually potent enantioselective and photoreactive barbiturate general anesthetic. *J. Med. Chem.* **55,** 6554–6565 CrossRef Medline

34. Jayakar, S. S., Zhou, X., Savechenkov, P. Y., Chiara, D. C., Desai, R., Bruzik, K. S., Miller, K. W., and Cohen, J. B. (2015) Positive and negative allosteric modulation of an $\alpha1\beta3\gamma2$ γ-aminobutyric acid type A (GABA_A) receptor by binding to a site in the transmembrane domain at the γ^+-β^- interface. *J. Biol. Chem.* **290,** 23432–23446 CrossRef Medline

35. Brauer, A. W., Oman, C. L., and Margolies, M. N. (1984) Use of *o*-phthalaldehyde to reduce background during automated Edman degradation. *Anal. Biochem.* **137,** 134–142 CrossRef Medline

36. Middleton, R. E., and Cohen, J. B. (1991) Mapping of the acetylcholine binding site of the nicotinic acetylcholine receptor: [³H]nicotine as an agonist photoaffinity label. *Biochemistry* **30,** 6987–6997 CrossRef Medline

37. Hill-Venning, C., Peters, J. A., Callachan, H., Lambert, J. J., Gemmell, D. K., Anderson, A., Byford, A., Hamilton, N., Hill, D. R., Marshall, R. J., and Campbell, A. C. (1996) The anaesthetic action and modulation of GABA_A receptor activity by the novel water-soluble aminosteroid Org 20599. *Neuropharmacology* **35,** 1209–1222 CrossRef Medline

38. Carter, R. B., Wood, P. L., Wieland, S., Hawkinson, J. E., Belelli, D., Lambert, J. J., White, H. S., Wolf, H. H., Mirsadeghi, S., Tahir, S. H., Bolger, M. B., Lan, N. C., and Gee, K. W. (1997) Characterization of the anticon-

vulsant properties of ganaxolone (CCD 1042; 3α-hydroxy-3β-methyl-5α-pregnan-20-one), a selective, high-affinity, steroid modulator of the γ-aminobutyric acid(A) receptor. *J. Pharmacol. Exp. Ther.* **280,** 1284–1295 Medline

39. Martinez Botella, G., Salituro, F. G., Harrison, B. L., Beresis, R. T., Bai, Z., Blanco, M. J., Belfort, G. M., Dai, J., Loya, C. M., Ackley, M. A., Althaus, A. L., Grossman, S. J., Hoffmann, E., Doherty, J. J., and Robichaud, A. J. (2017) Neuroactive steroids. 2. 3a-hydroxy-3b-methyl-21-(4-cyano-1H-pyrazol-1'-yl)-19-nor-5b-pregnan-20-one (SAGE-217): a clinical next generation neuroactive steroid positive allosteric modulator of the (γ-aminobutyric acid)A receptor. *J. Med. Chem.* **60,** 7810–7819 CrossRef Medline

40. Edgar, D. M., Seidel, W. F., Gee, K. W., Lan, N. C., Field, G., Xia, H., Hawkinson, J. E., Wieland, S., Carter, R. B., and Wood, P. L. (1997) CCD-3693: an orally bioavailable analog of the endogenous neuroactive steroid, pregnanolone, demonstrates potent sedative hypnotic actions in the rat. *J. Pharmacol. Exp. Ther.* **282,** 420 Medline

41. Hogenkamp, D. J., Tran, M. B., Yoshimura, R. F., Johnstone, T. B., Kanner, R., and Gee, K. W. (2014) Pharmacological profile of a 17β-heteroaryl-substituted neuroactive steroid. *Psychopharmacology* **231,** 3517–3524 CrossRef Medline

42. Tsai, S. E., Lee, J. C., Uramaru, N., Takayama, H., Huang, G. J., and Wong, F. F. (2017) Synthesis and antiproliferative activity of 3α-hydroxy-3β-methoxymethyl-5α-pregnan-20-one with a C-21 hydrophilic substituent. *Heteroatom. Chem.* **28,** e21372 CrossRef

43. Belelli, D., Lambert, J. J., Peters, J. A., Gee, K. W., and Lan, N. C. (1996) Modulation of human recombinant GABA_A receptors by pregnanediols. *Neuropharmacology* **35,** 1223–1231 CrossRef Medline

44. Ziegler, E., Bodusch, M., Song, Y., Jahn, K., Wolfes, H., Steinlechner, S., Dengler, R., Bufler, J., and Krampfl, K. (2009) Interaction of androsterone and progesterone with inhibitory ligand-gated ion channels: a patch clamp study. *Naunyn-Schmiedebergs Arch. Pharmacol.* **380,** 277–291 CrossRef Medline

45. Savechenkov, P. Y., Chiara, D. C., Desai, R., Stern, A. T., Zhou, X. N., Ziemba, A. M., Szabo, A. L., Zhang, Y., Cohen, J. B., Forman, S. A., Miller, K. W., and Bruzik, K. S. (2017) Synthesis and pharmacological evaluation of neurosteroid photoaffinity ligands. *Eur. J. Med. Chem.* **136,** 334–347 CrossRef Medline

46. Mascia, M. P., Asproni, B., Busonero, F., Talani, G., Maciocco, E., Pau, A., Cerri, R., Sanna, E., and Biggio, G. (2005) Ethyl 2-(4-bromophenyl)-1-(2,4-dichlorophenyl)-1H-4-imidazolecarboxylate is a novel positive modulator of GABA_A receptors. *Eur. J. Pharmacol.* **516,** 204–211 CrossRef Medline

47. Lynagh, T., and Lynch, J. W. (2012) Ivermectin binding sites in human and invertebrate Cys-loop receptors. *Trends Pharmacol. Sci.* **33,** 432–441 CrossRef Medline

48. Hibbs, R. E., and Gouaux, E. (2011) Principles of activation and permeation in an anion-selective Cys-loop receptor. *Nature* **474,** 54–60 CrossRef Medline

49. Estrada-Mondragon, A., and Lynch, J. (2015) Functional characterization of ivermectin binding sites in $\alpha1\beta2\gamma2L$ GABA_A receptors. *Front. Mol. Neurosci.* **8,** 55 CrossRef Medline

50. Reddy, D. S., and Jian, K. H. (2010) The testosterone-derived neurosteroid androstanediol is a positive allosteric modulator of GABA_A receptors. *J. Pharm. Exp. Ther.* **334,** 1031–1041 CrossRef Medline

51. Hawkinson, J. E., Kimbrough, C. L., Belelli, D., Lambert, J. J., Purdy, R. H., and Lan, N. C. (1994) Correlation of neuroactive steroid modulation of [³⁵S]*t*-butylbicyclophosphorothionate and [³H]flunitrazepam binding and γ-aminobutyric acid_A receptor function. *Mol. Pharmacol.* **46,** 977–985 Medline

52. Katona, B. W., Krishnan, K., Cai, Z. Y., Manion, B. D., Benz, A., Taylor, A., Evers, A. S., Zorumski, C. F., Mennerick, S., and Covey, D. F. (2008) Neurosteroid analogues: 12. potent enhancement of GABA-mediated chloride currents at GABA_A receptors by *ent*-androgens. *Eur. J. Med. Chem.* **43,** 107–113 CrossRef Medline

53. Prince, R. J., and Simmonds, M. A. (1992) 5β-Pregnan-3β-ol-20-one, a specific antagonist at the neurosteroid site of the GABA_A receptor-complex. *Neurosci. Lett.* **135,** 273–275 CrossRef Medline

54. Maitra, R., and Reynolds, J. N. (1998) Modulation of GABA_A receptor function by neuroactive steroids: evidence for heterogeneity of steroid

sensitivity of recombinant GABA~A~ receptor isoforms. *Can. J. Physiol. Pharmacol.* **76,** 909–920 CrossRef Medline

55. Garrett, K. M., and Gan, J. (1998) Enhancement of γ-aminobutyric acid~A~ receptor activity by α-chloralose. *J. Pharmacol. Exp. Ther.* **285,** 680–686 Medline

56. Wang, M.-D., Rahman, M., Zhu, D., Johansson, I.-M., and Bäckström, T. (2007) 3β-Hydroxysteroids and pregnenolone sulfate inhibit recombinant rat GABA~A~ receptor through different channel property. *Eur. J. Pharmacol.* **557,** 124–131 CrossRef Medline

57. Turner, D. M., Ransom, R. W., Yang, J. S. J., and Olsen, R. W. (1989) Steroid anesthetics and naturally occurring analogs modulate the γ-aminobutyric acid receptor complex at a site distinct from barbiturates. *J. Pharmacol. Exp. Ther.* **248,** 960–966 Medline

58. Prince, R. J., and Simmonds, M. A. (1993) Differential antagonism by epipregnanolone of alphaxalone and pregnanolone potentiation of [³H]flunitrazepam binding suggests more than one class of binding site for steroids at GABA~A~ receptors. *Neuropharmacology* **32,** 59–63 CrossRef Medline

59. Kelley, S. P., Alan, J. K., O'Buckley, T. K., Mennerick, S., Krishnan, K., Covey, D. F., and Leslie Morrow, A. (2007) Antagonism of neurosteroid modulation of native γ-aminobutyric acid receptors by (3α,5α)-17-phenylandrost-16-en-3-ol. *Eur. J. Pharmacol.* **572,** 94–101 CrossRef Medline

60. Goodnough, D. B., and Hawkinson, J. E. (1995) Neuroactive steroid modulation of [³H]muscimol binding to the GABA~A~ receptor complex in rat cortex. *Eur. J. Pharmacol.* **288,** 157–162 CrossRef

61. Rahman, M., Lindblad, C., Johansson, I. M., Backstrom, T., and Wang, M. D. (2006) Neurosteroid modulation of recombinant rat α5β2γ2L and α1β2γ2L GABA~A~ receptors in *Xenopus* oocyte. *Eur. J. Pharmacol.* **547,** 37–44 CrossRef Medline

62. Jayakar, S. S., Zhou, X., Chiara, D. C., Dostalova, Z., Savechenkov, P. Y., Bruzik, K. S., Dailey, W., Miller, K. W., Eckenhoff, R. G., and Cohen, J. B. (2014) Multiple propofol-binding sites in a γ-aminobutyric acid type A receptor (GABA~A~R) identified using a photoreactive propofol analog. *J. Biol. Chem.* **289,** 27456–27468 CrossRef

63. Dostalova, Z., Liu, A. P., Zhou, X. J., Farmer, S. L., Krenzel, E. S., Arevalo, E., Desai, R., Feinberg-Zadek, P. L., Davies, P. A., Yamodo, I. H., Forman, S. A., and Miller, K. W. (2010) High-level expression and purification of Cys-loop ligand-gated ion channels in a tetracycline-inducible stable mammalian cell line: GABA~A~ and serotonin receptors. *Protein Sci.* **19,** 1728–1738 CrossRef Medline

64. Dostalova, Z., Zhou, X., Liu, A., Zhang, X., Zhang, Y., Desai, R., Forman, S. A., and Miller, K. W. (2014) Human α1β3γ2L γ-aminobutyric acid type A receptors: high-level production and purification in a functional state. *Protein Sci.* **23,** 157–166 CrossRef

65. Scott, M. G., Crimmins, D. L., McCourt, D. W., Tarrand, J. J., Eyerman, M. C., and Nahm, M. H. (1988) A simple in situ cyanogen bromide cleavage method to obtain internal amino acid sequence of proteins electroblotted to polyvinyldifluoride membranes. *Biochem. Biophys. Res. Commun.* **155,** 1353–1359 CrossRef Medline

66. Hamouda, A. K., Kimm, T., and Cohen, J. B. (2013) Physostigmine and galanthamine bind in the presence of agonist at the canonical and noncanonical subunit interfaces of a nicotinic acetylcholine receptor. *J. Neurosci.* **33,** 485–494 CrossRef Medline

67. Li, P., Bandyopadhyaya, A. K., Covey, D. F., Steinbach, J. H., and Akk, G. (2009) Hydrogen bonding between the 17β-substituent of a neurosteroid and the GABA~A~ receptor is not obligatory for channel potentiation. *Br. J. Pharmacol.* **158,** 1322–1329 CrossRef Medline

68. Slavíková, B., Bujons, J., Matyás, L., Vidal, M., Babot, Z., Kristofikova, Z., Suñol, C., and Kasal, A. (2013) Allopregnanolone and pregnanolone analogues modified in the C ring: synthesis and activity. *J. Med. Chem* **56,** 2323–2336 CrossRef Medline

69. Nourmahnad, A., Stern, A. T., Hotta, M., Stewart, D. S., Ziemba, A. M., Szabo, A., and Forman, S. A. (2016) Tryptophan and cysteine mutations in M1 helices of α1β3γ2L γ-aminobutyric acid type A receptors indicate distinct intersubunit sites for four intravenous anesthetics and one orphan site. *Anesthesiology* **125,** 1144–1158 CrossRef Medline

ASBMB